AN ABSTRACT OF THE THESIS OF

Pedro Lee (Name) for the M.S. (Degree) in Electrical and Electronics Engineering (Major)

Date thesis is presented Sept. 30, 1966

Title INVESTIGATION OF SPECIAL MAGNETIC MEMORY DEVICES

Redacted for Privacy

Abstract approved _____ (Major professor)

Three types of magnetic memory elements with emphasis placed on low cost and batch fabrication are investigated. The type I element consists of a wired hole in a strip of Deltamax tape. The type II element uses a stack of magnetic tape instead of the Deltamax. The type III element consists of a pre-wired grid with magnetic material deposited around the grid to simulate a wired core. The results obtained from these investigations showed conclusively that the type I element, referred to as apertured Deltamax memory cell in this paper, operates satisfactorily as a memory element. The fabrication technology is based on etching small holes through a thin Deltamax tape to form memory cells. The operation of the uncompensated and compensated memory cell is investigated. Oscillograms and graphs of the typical characteristics response of the memory cell are presented, and a qualitative description given.

The type II and type III elements are found

incapable of operating as a memory device because of the magnetic properties of the available tape and magnetic powder. Summaries of type II and III elements are given in Appendix I and II respectively.

INVESTIGATION OF SPECIAL MAGNETIC MEMORY DEVICES

by

PEDRO LEE

A THESIS

submitted to

OREGON STATE UNIVERSITY

in partial fulfillment of
the requirements for the
degree of

MASTER OF SCIENCE

June 1967

APPROVED:

Redacted for Privacy

Professor of Electrical and Electronics Engineering
In Charge of Major

Redacted for Privacy

Head of Department of Electrical and Electronics Engineering

Redacted for Privacy

Dean of Graduate School

Date thesis is presented Sept. 30, 1966

Typed by Erma McClanathan

ACKNOWLEDGMENT

The author wishes to express appreciation to Professor L. N. Stone for his suggestion of the thesis topic, and also for his continuous encouragement throughout the experimental work and the writing of this thesis.

TABLE OF CONTENTS

LIST OF FIGURES

Figure

Figure

LIST OF TABLES

INVESTIGATION OF SPECIAL MAGNETIC MEMORY DEVICES

INTRODUCTION

There is a growing need for computer memories compatible with the faster, smaller, cheaper integrated circuit packages now being used in digital computers. Because of this need, computer manufacturers are demanding something better than wire-threaded ferrite core memories.

Large matrix memories containing millions of cores are expensive to construct. A major part of the production cost results from labor involved in core-by-core hand wiring. Any system which significantly reduces this labor expense would be attractive. Three methods have been investigated and will be discussed.

1. The type I element consisted of a wire passing through a hole in a strip of Deltamax tape. Deltamax is a grain-oriented 50 percent nickel-iron alloy having a rectangular hysteresis loop. The magnetic material adjacent to the hole is used in a manner similar to the material in a toroidal core. Holes were chemically etched through the thin metal tape. The etching process is particularly suited for automation.

Each strip of metal tape may contain a large number of holes. Therefore, the number of separate components to be handled during assembly is drastically reduced.

The type I element proved to be feasible as a memory device. The operation of this element will be discussed and documented in this paper.

2. The type II element used a stack of magnetic tape instead of the Deltamax tape of the type I element. Unlike the type I element, the holes and its wiring may be inserted by a machine similar to a sewing machine. From the results obtained, the type II element did not accomplish its objective as a memory device. Information concerning type II element can be found in Appendix I.

3. The type III element consisted of a grid of word-drive and digit-sense wires surrounded by a packed magnetic powder. This type of memory eliminates the costly process of threading wires through tiny toroidal cores. Because of improper magnetic powder and method used to deposit it on the grid, no results were obtained for the type III element. Information concerning type III element can be found in Appendix II.

I. TYPE I ELEMENT:
APERTURED DELTAMAX MEMORY CELL

1. Nomenclature and Definitions

Nomenclature

F = Magnetomotive force, ampere-turn.
H_c = Coercive force, oersted.
H = Applied magnetic field strength, oersted.
B_r = Remanent flux density, gauss.
B_s = Saturation flux density, gauss.
ϕ = Magnetic flux, maxwell.
ϕ_r = Reversible magnetic flux, maxwell.
μ_s = Saturation permeability, no unit.
ρ = Constant of magnetic material, $\frac{\text{centimeter}}{\text{second-oersted}}$.
r = Radius, centimeter.
h = Thickness, centimeter.
A = Cross section area, centimeter^2.
N_d = Number of turns in the drive winding.
I_R = Read current, ampere.
I_w = Write current, ampere.
I_c = Compensation current, ampere.
t_r = Pulse rise time, second.
t_f = Pulse fall time, second.
t_s = Pulse storage time, second.
t_d = Pulse width, second.
t_s = Switching time, second.
t_p = Peaking time, second.
t_c = Cycle time, second.
uV_1 = "Undisturbed 1" sense-winding voltage, volt.
uV_z = "Undisturbed 0" sense-winding voltage, volt.
cV_1 = Compensated "undisturbed 1" sense-winding voltage, volt.
cV_z = Compensated "undisturbed 0" sense-winding voltage, volt.
$uV_z@t_p$ = "Undisturbed 0" sense-winding voltage measured at t_p, volt.
$cV_z@t_p$ = Compensated "undisturbed 0" sense-winding voltage measured at t_p, volt.

Definitions

Write Current (I_w). The peak value of a negative going current pulse required to switch the memory cell from its "0" state to its "1" state.

Read Current (I_R). The peak value of a positive going current pulse required to switch the memory cell from its "1" state to its "0" state.

Compensation Current (I_C). The peak value of a positive going current pulse required to drive the compensation cell from its "0" state further into saturation.

"Undisturbed 1" Sense-Winding Voltage (uV_1). The peak value of the output voltage produced when an uncompensated memory cell, which is in its "undisturbed 1" state, is subjected to a "read" current pulse having a peak value I_R.

"Undisturbed 0" Sense-Winding Voltage (uV_z). The peak value of the output voltage produced when an uncompensated memory cell, which is in its "undisturbed 0" state, is subjected to a "read" current pulse having a peak value of I_R.

Compensated "Undisturbed 1" Sense-Winding Voltage (cV_1). The peak value of the output voltage produced when a compensated memory cell, which is in its "undisturbed 1" state, is subjected to a "read" current pulse having a

peak value of I_R.

Compensated "Undisturbed 0" Sense-Winding Voltage (cV_z). The peak value of the output voltage produced when a compensated memory cell, which is in its "undisturbed 0" state, is subjected to a "read" current pulse having a peak value of I_R.

Pulse Rise Time (t_r). The time interval between the time at which the driving current reaches to ten percent of its peak value and the time it reaches to 90 percent of its peak value.

Pulse Fall Time (t_f). The time interval between the time at which the driving current falls to ten percent of its peak value and the time at which it falls to 90 percent of its peak value.

Pulse Duration (t_d). The time interval between the time at which the driving current rises to 90 percent of its peak value and the time at which it falls to 90 percent of its peak value.

Switching Time (t_s). The time interval between the time at which the driving current rises to ten percent of its peak value and the time at which the "undisturbed 1" response voltage decays to ten percent of its peak value.

Peaking Time (t_p). The time interval between the time at which the driving current rises to ten percent

of its peak value and the time at which the "undisturbed 1" response voltage reaches its peak value.

2. Principle of Operation of the Apertured Deltamax Memory Cell

The principle of operation of a memory cell can be described more effectively by comparing it with that of a toroidal core. Take, for example, an unmagnetized toroidal core of a rectangular dynamic magnetization loop material with dimensions shown in Figure 1(a), and an unmagnetized memory cell of the same material with the dimensions shown in Figure 1(b). Suppose that both are subjected to a magnetomotive force, gradually increasing from zero, applied by means of a winding passing through the center of the core and the memory cell. There is no change of flux until the applied field becomes equal to the coercive field for the material. If the material has an ideal rectangular dynamic magnetization loop, the flux change will first occur at the inner wall of both the core and the memory cell, when the applied magnetomotive force reaches the value of

$$F_1 = 5H_c r_1 \tag{2.1}$$

F = magnetomotive force, ampere-turn

H_c = coercive force, oersted

r_1 = inner radius, centimeter

The flux change moves outward as the magnetomotive force increases (see Figure 2). When the magnetomotive

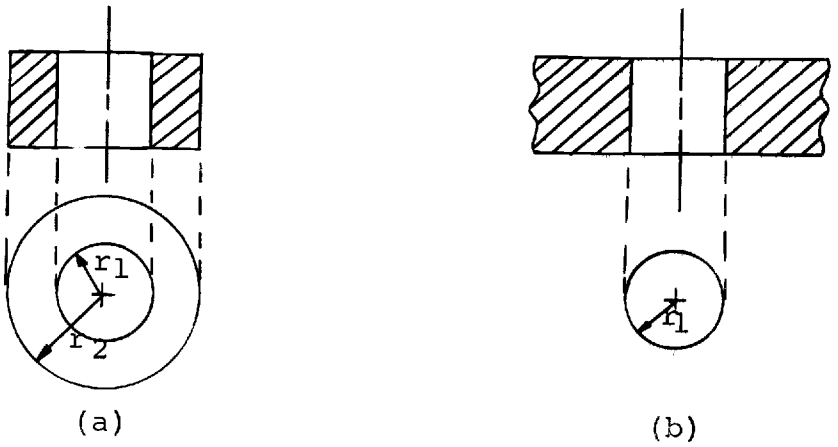

Figure 1. Geometry of (a) toroidal core,
(b) memory cell.

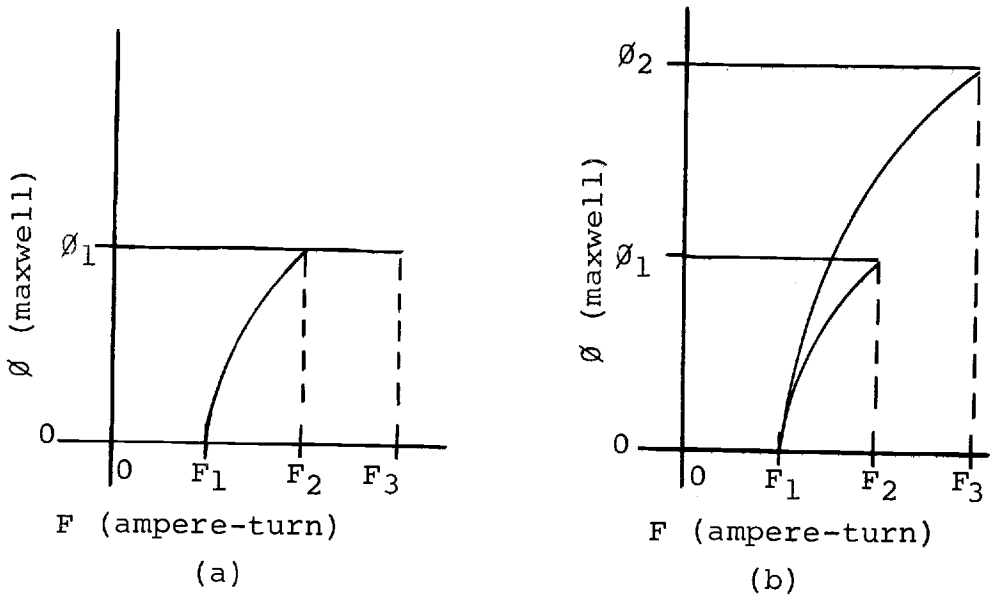

Figure 2. Initial magnetizing characteristic.

(a) Toroidal core
(b) Memory cell

force reaches the value,

(2.2) $F_2 = 5H_c r_2$ r_2 = core's outer radius, centimeter

all the material of the core is saturated. Upon the removal of the applied field, the remanent flux of both the core and the memory cell is

(2.3) $\phi_1 = AB_r$ ϕ = magnetic flux, maxwell

$= (r_2 - r_1)\, hB_r$ B_r = remanent flux density, gauss

A = cross section area, centimeter^2

h = thickness, centimeter

For the memory cell a further increase in magneto-motive force to F_3 will cause the flux to spread to a radius r_3,

(2.4) $r_3 = \frac{F_3}{5H_c}$ $r_3 > r_2$.

The remanent flux of the memory cell upon the removal of the excitation is

(2.5) $\phi_2 = (r_3 - r_1)\, hB_r$.

The remanent flux of the core, on the other hand, remains to be

(2.6) $\phi_1 = (r_2 - r_1)\, hB_r$.

The spread of remanent flux is limited by the outer wall of the core. The excess of the applied magneto-motive force will simply drive the core further into saturation.

The spread of remanent flux in a memory cell

depends on the applied field and is not limited by an outer wall as is the core.

From Figure 2(b), which shows the initial magnetizing characteristic for the memory cell, it can be noted that the dynamic magnetization loop for the memory cell becomes less rectangular as the spread of remanent flux increases.

The "1" and "0" are stored in the toroidal core by the two states of equal but opposite remanence.

The "0" state in a memory cell is represented by a penetration of flux of one polarity to a certain radius, and the "1" state to an opposite penetration to a certain radius.

The sense windings, coupled with the magnetic path in both cases, can detect the information stored in the form of the electromotive force generated by the flux change.

3. Magnetic Properties of Deltamax

Deltamax is a grain-oriented 50 percent nickel-iron alloy, with a dynamic magnetization loop at least as square as any which has yet been attained with ferrites.

Deltamax is available only in the form of thin tape ranging from 1 mil to 4 mils in thickness, because of the severe cold-reduction necessary to achieve its

magnetic properties, and also owing to its high conductivity, the Deltamax tape must be rolled within this range in order to reduce the eddy-current loss to an acceptable level.

Deltamax is strain sensitive. Depreciation of its magnetic properties can be caused either by handling or by wire winding.

Figure 31 (Appendix IV) shows the dynamic magnetization loops of Deltamax. The remanence is approximately 14,000 gauss compared to 2,000 to 3,000 gauss for ferrite. The coercive force is 0.2 to 0.4 oersteds as compared to 0.6 to 3 oersteds for ferrite. The low coercivity and high remanence of Deltamax lead to lower drive current and higher sense voltage than ferrite. The squareness ratio of Deltamax is approximately

$$\text{Squareness ratio at 60 cycles A.C.} = \frac{B_{\alpha}}{B_m} = \frac{13{,}800 \text{ gauss}}{14{,}000 \text{ gauss}} \cong 1$$

where B_m is the flux density level produced by a field H_m sufficient to switch the core from one remanent state to the other, and B_{α} is the flux density level produced by a field $-H_m/2$ insufficient to cause any significant change of flux. Fields H_m and $-H_m/2$ at 60 cycles A.C. are 0.4 and -0.2 oersted respectively as shown in Figure 31 (Appendix IV). The near unity squareness ratio obtained for Deltamax exceeds that of ferrite, and

consequently the half selected noise produced by a Deltamax core is lower than that of a ferrite core.

Figure 32 (Appendix IV) shows the effect of temperature on the dynamic magnetization loop of Deltamax at 60 cycles A.C. It may be noted that the values of coercive force decrease for temperatures above room temperature, and increase for temperature below room temperature. The change of flux density with temperature is small; it decreases for temperatures above and below room temperature.

4. Construction of Apertured Deltamax Memory Cell

Strips of Deltamax tape with thickness of two and four mils were extracted from metal tape core available in the laboratory. Since the material is stress sensitive, holes were chemically etched through the tape, instead of punching or drilling. Holes eight mils in diameter spaced 30 mils from center to center were etched. The proper procedure for this deep etching, also called "chemical milling", of Deltamax tape is not known. The best result obtained after running several etching tests are shown in Figure 3. It may be noted that the etched pattern shows some imperfections. Figure 3(a) shows an over-etched hole, which damaged the surrounding material, and Figure 3(b) shows a portion of the tape

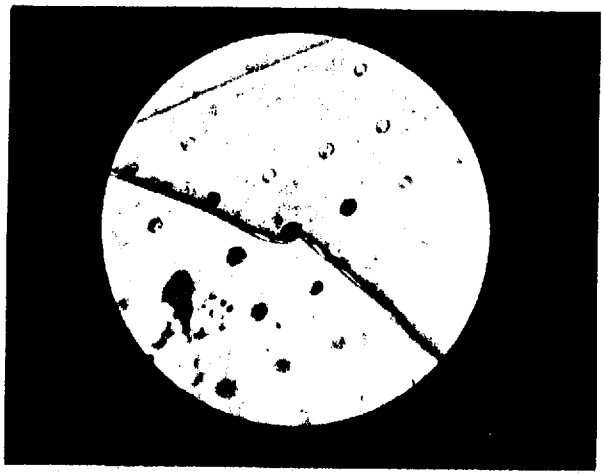

(a)

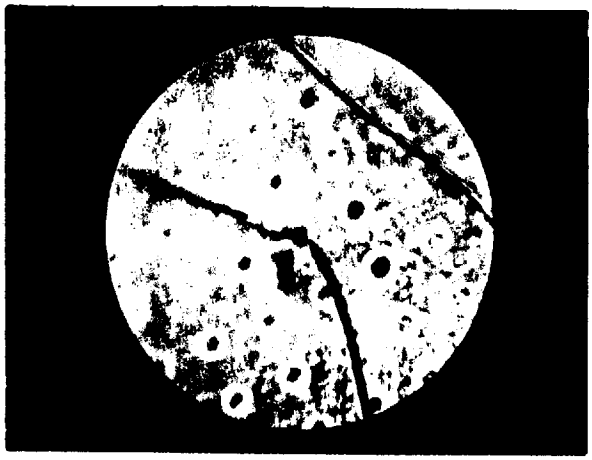

(b)

Magnification: X10

Figure 3. Top views of the etched holes on a Deltamax tape.

a) Shows an over-etched hole and the selected hole.
b) Holes not etched through, and the selected hole.

where some of the holes are not etched completely through the metal. Note also that some of the holes are not well defined. In addition to these imperfections, the tape thickness was reduced to about one mil during the etching process. The finished sample, however, served its purpose for the investigation of the apertured Deltamax memory cell. Undamaged portions of the tape with holes of good definition were selected.

Figure 4 shows the geometry of type I element. The cell's inner radius is four mils and the outer radius, limited by the adjacent holes, is 26 mils.

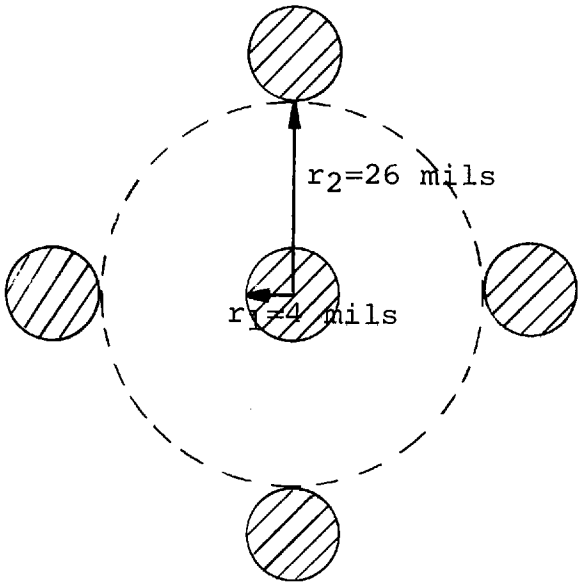

Figure 4. Geometry of type I element (apertured Deltamax memory cell).

Because of the low coercivity and high flux density of Deltamax tape, single-turn drive and sense windings were used.

A detailed description of the etching procedures used can be found in Appendix V. The important factors involved in each step of the process are discussed. In the conclusion of Appendix V, problems encountered in the etching process are analyzed and possible improvements are suggested.

5. Operation of the Uncompensated, Apertured Deltamax Memory Cell

A system diagram of the uncompensated, apertured Deltamax memory cell is shown in Figure 5. The term "uncompensated" is used here to differentiate from the compensated memory cell discussed in the next section.

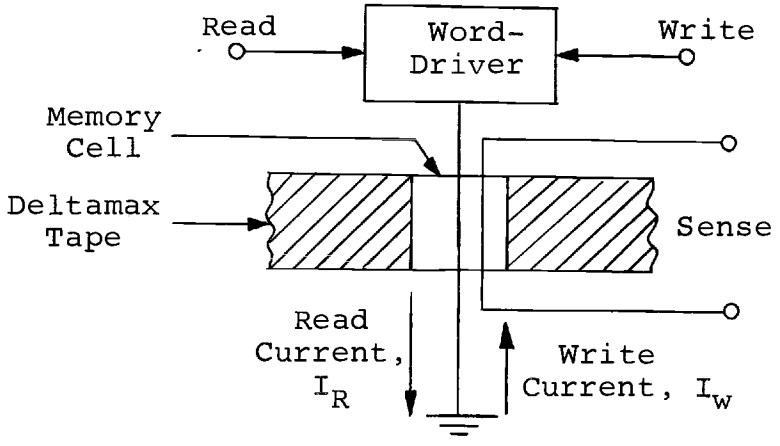

Figure 5. System diagram of the uncompensated, apertured Deltamax memory cell.

The read and write current pulses from the word-driver described in Appendix III were used to drive the memory cell. To study the response of the uncompensated memory cell, the read and write currents were increased to 800 milliamperes, where sizable sense-winding outputs were obtained as shown in Figure 6. Figure 6(a) shows a read "undisturbed 1" sense-winding output, uV_1, with a peak voltage of 35 millivolts at a peaking time, t_p, of 0.15 microsecond, and a switching time, t_s, of 1.3 microseconds. A "nonswitching" voltage, due to reversible flux change from "0" saturation state to its remanence state, occurred in the form of a negative peak of 28 millivolts on the fall of the read current pulse. By removing the write pulse, a read "undisturbed 0" sense-winding output, uV_z, was obtained as shown in Figure 6(b). The output shows two "nonswitching" voltages in the form of positive and negative peaks of 25 millivolts. The positive peak voltage was generated by the reversible flux change from the "0" remanence state to its saturation state on the rise of the applied read current pulse. The negative peak voltage was generated by the reversible flux change from the "0" saturation state back to its remanence state on the fall of the applied read current pulse. The nearly equal areas under the positive and negative peaks testify that there was no net change in

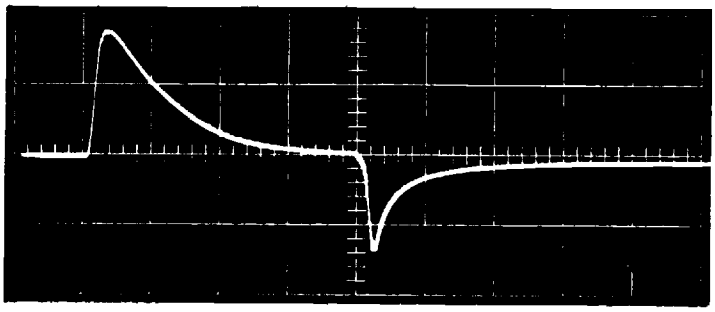

(a)

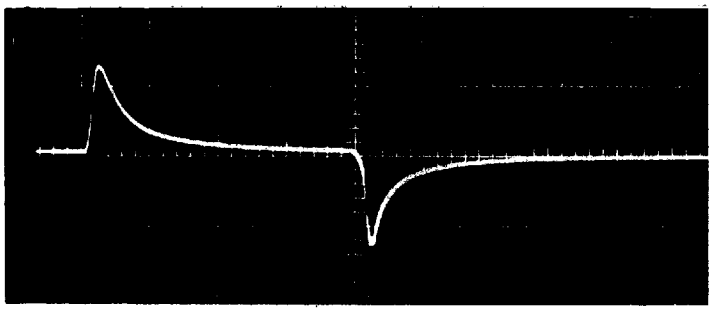

(b)

Scale: Horizontal = 0.5 microseconds per division.
Vertical = 20 millivolts per division.

Figure 6. Sense-winding voltages from the uncompensated, apertured Deltamax memory cell.

a) Uncompensated "undisturbed 1", uV_1.
b) Uncompensated "undisturbed 0", uV_z.

Write drive ($N_d I_w$) = 800 milliampere-turns
Read drive ($N_d I_R$) = 800 milliampere-turns
Pulse rise time (t_r) = 0.15 microsecond
Pulse fall time (t_f) = 0.1 microsecond
Pulse width (t_d) = 2 microseconds
Frequency = 1 kilocycle

flux, which indicates that the memory cell was switched without changing its state.

The recorded sense-winding output waveforms for the memory cell are rather similar to that of a toroidal ferrite core, except for a very long "tail" and fairly large "nonswitching" signals. The long "tail" after the peak voltage can be explained by considering the rate at which the flux penetrates the surrounding material when magnetomotive force is applied. From Section 2, it can be seen that, when the magnetic saturation of material around the hole is reversed by means of a current pulse, a cylindrical boundary may be imagined to move outward from the circumference of the hole. Switching is completed inside the boundary, and no irreversible switching takes place outside this boundary. The differential equation, which expresses the penetration of the boundary of radius r into the material as a function of time t, can be shown (3, p. 1023; 12, p. 455) to be

$$(5.1)\quad \frac{dr}{dt} = \rho(H-H_c) = \rho\left(\frac{IN_d}{5r} - H_c\right)$$

ρ = constant of material, $\frac{\text{centimeter}}{\text{second-oersted}}$

H = applied field strength, oersted

H_c = coercive force of the material, oersted

I = drive current, ampere

N_d = 1, number of turns in the drive winding

r = boundary radius, centimeter.

The solution to this equation is

$$(5.2)\quad I \log \frac{I - 5H_c r_1}{I - 5H_c r} - 5H_c(r - r_1) = 5\rho H_c^2 t.$$

Let $r_m = \frac{I}{5H_c}$ we can solve for r,

$$(5.3)\quad r = r_m \left[1 - (1 - \frac{r_1}{r_m})\, e^{-\rho H_c t / r_m}\ e^{-r/r_m}\ e^{r_1/r_m} \right]$$

r = boundary radius r at time t, centimeter

r_1 = initial radius, centimeter.

If the penetration of the boundary radius r with time t is plotted from the above expression, a curve of the type shown in Figure 7 is obtained. The curve is

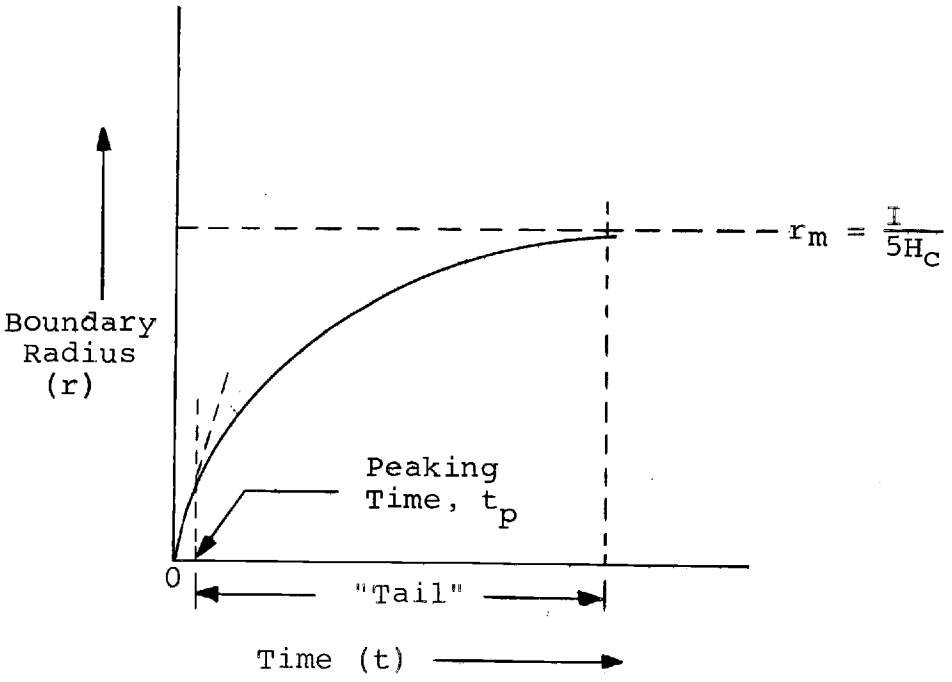

Figure 7. Penetration of flux reversal in term of boundary radius (r), as function of time (t).

essentially an exponential rise of the boundary penetration radius r to a final value of

$$(5.4) \quad r_m = \frac{I}{5H_c} \text{ at } t = \infty \ .$$

It may be noted from Figure 7 that the maximum slope or maximum rate of flux change ends at the peaking time, t_p, where the output voltage reaches maximum value. After t_p, the slope of the curve starts to decrease gradually toward zero; so does the output sense voltage. This gradual decrease in the output voltage is shown in Figure 6(a) as a long tail after t_p. As shown in Figure 7, the peaking time, t_p, and the peak output voltage depend on the initial slope of the penetration curve. Note also from Figures 6(a) and 7 that the switching time, t_s, depends almost entirely on the decay time of the long tail.

The large "nonswitching" outputs that are shown in Figure 6 are caused by the bulk material surrounding the hole, which contributes to a large reversible flux change. Let us consider a memory cell with a hole of radius r_1, and the outer radius limited to r_2. The reversible flux change in a section of width Δr caused by a current pulse I is

$$(5.5)\quad \Delta\phi_r = \mu_s H h \Delta r = \mu_s h \Delta r \frac{IN_d}{5r}$$

where $\Delta\phi_r$ = reversible flux change in a section width Δr, maxwell

μ_s = saturation permeability, no unit

h = thickness of the material, centimeter

H = applied magnetic field strength, oersted

N_d = 1, number of turns in the drive winding.

By integrating $\Delta\phi_r$ from the inner radius r_1 to the outer radius r_2, the total reversible flux change of the memory cell is

$$(5.6)\quad \phi_r = \frac{\mu_s I h}{5} \int_{r=r_1}^{r=r_2} \frac{1}{r}\, dr$$

$$= \frac{\mu_s I h}{5} \left(\log \frac{r_2}{r_1}\right)$$

where ϕ_r = total reversible flux change, maxwell.

From the total reversible flux change expression, the influence of the bulk material around the hole is shown as the ratio $\frac{r_2}{r_1}$. The memory cell used has the dimensions shown in Figure 4. This gives the ratio,

$$\beta = \frac{r_2}{r_1} = \frac{26 \text{ mils}}{4 \text{ mils}} = 6.5$$

where r_2 = effective outside radius, centimeter

r_1 = inner radius, centimeter

β = ratio of outer and inner radius.

The value of β for most toroidal cores ranges from 1.5 to 1.7. The reversible flux changes of memory cell, and toroidal cores of the same material are in the ratio

$$\log 6.5 : \log 1.7$$

$$= 3.5 : 1$$

Therefore, the "nonswitching" signals from the memory cell are about 3.5 times as large as those from a toroidal core of similar material. By placing the holes near an edge of the tape, or placing them near to each other, the bulk material surrounding each hole can be minimized, and in the same manner the "nonswitching" signals can be reduced. An optimum spacing of twice their diameter between centers of the holes has been suggested (11, p. 385). This distance is a compromise between discrimination improvement and interaction between holes.

Typical characteristics of an uncompensated, apertured Deltamax memory cell were obtained as shown in Figure 8 (Table 2). The effect of the read pulse on the sense-winding output voltage was observed. A write pulse of 800 milliamperes was used to completely saturate the memory cell after each read operation.

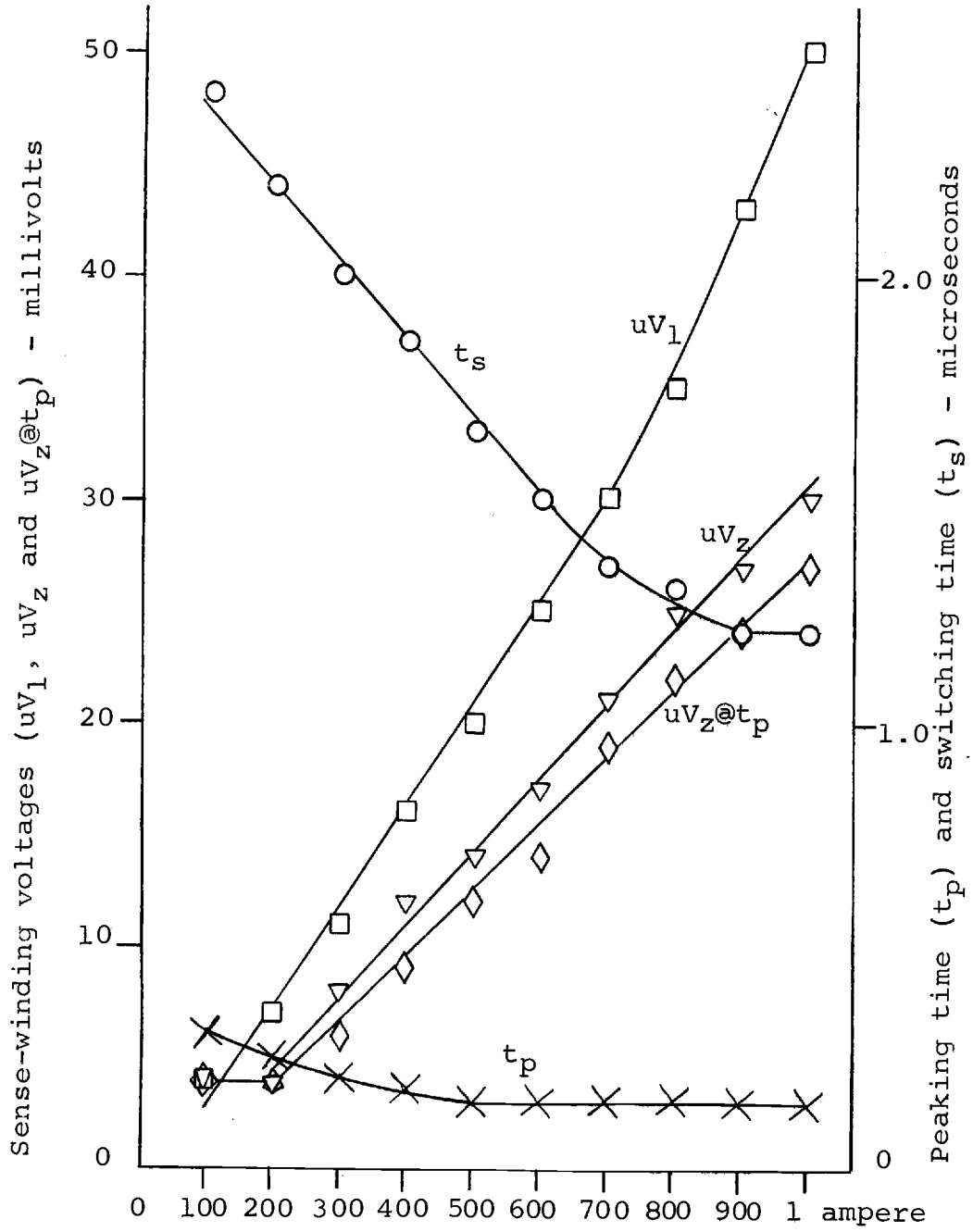

Figure 8. Typical characteristics for the uncompensated, apertured Deltamax memory cell.

(See Table II, Appendix VI for test conditions)

Several facts can be observed from the curves in Figure 8. The switching time, t_s, decreased rapidly as the read current was increased and leveled off at about 800 milliamperes, while the peaking time, t_p, remained fairly constant. This shows that the variation of t_s is almost completely caused by the variation of the "tail" decay time. As discussed previously, the penetration of flux reversal curve in Figure 7 showed that the target radius,

$$r_m = \frac{I}{5H_c}$$

increases as the drive current increases. This results in a larger value for the curve's initial slope. With this increase of initial slope comes a smaller peaking time, t_p, and a large decrease of the "tail" decay time.

The increase of the "undisturbed 1" sense-winding voltage, uV_1, caused by the increase of read current, can be readily seen from the increase of the target radius and the increase of the rate of flux reversal penetration.

The increase of the "undisturbed 0" sense-winding voltage, uV_z, with the increase of read drive current, is due to the increase of reversible flux change in the memory cell caused by the large read current, as was shown in equation (5.6).

The "undisturbed 0" sense-winding output measured

at the t_p, uV_z @ t_p, shows the discrimination between read "1" and read "0", in case the output voltages were sampled by means of a strobe pulse at the peaking time of the uV_1 output.

In summarizing the foregoing analysis, the poor discrimination between "1" and "0" outputs constitutes the main disadvantage of the uncompensated, apertured Deltamax memory cell. From the curves in Figure 8, the largest ratio between "undisturbed 1" and "undisturbed "0" at t_p is only

$$\frac{uV_1}{uV_z \text{ @ } t_p} = \frac{50 \text{ millivolts}}{27 \text{ millivolts}} = 1.85$$

at the expense of a large read drive current of one ampere.

6. Operation of the Compensated, Apertured Deltamax Memory Cell

To improve the discrimination, a compensated memory cell was devised. The system consists of a storage cell and a compensation cell as shown in Figure 9.

The word driver was used to drive the storage cell as before. The compensation cell was driven by a compensation driver. The compensation driver is essentially half of the bridge circuit of the word driver described in Appendix III. The compensation driver generates a unipolar compensation current, I_c, in the read direction.

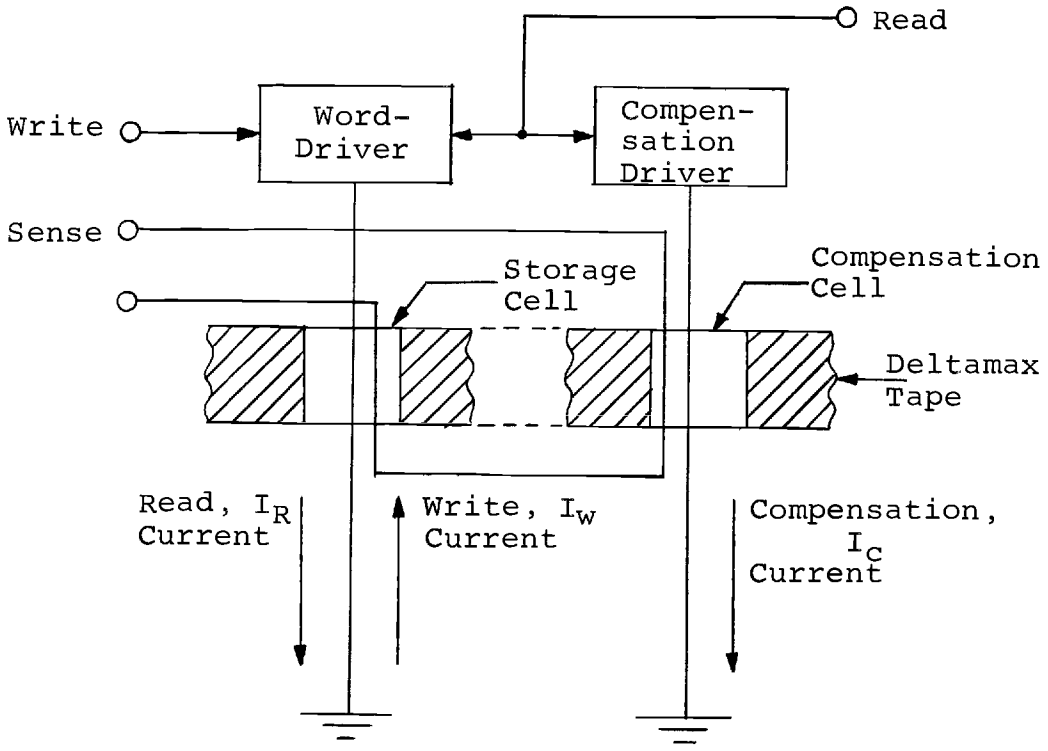

Figure 9. System diagram of the compensated, apertured Deltamax memory cell.

The sense winding was threaded through both cells, in such a way that the polarity of the induced sense-winding voltages from the storage cell and compensation cell are in opposition.

An ideal operation of compensation is shown in Figure 10.

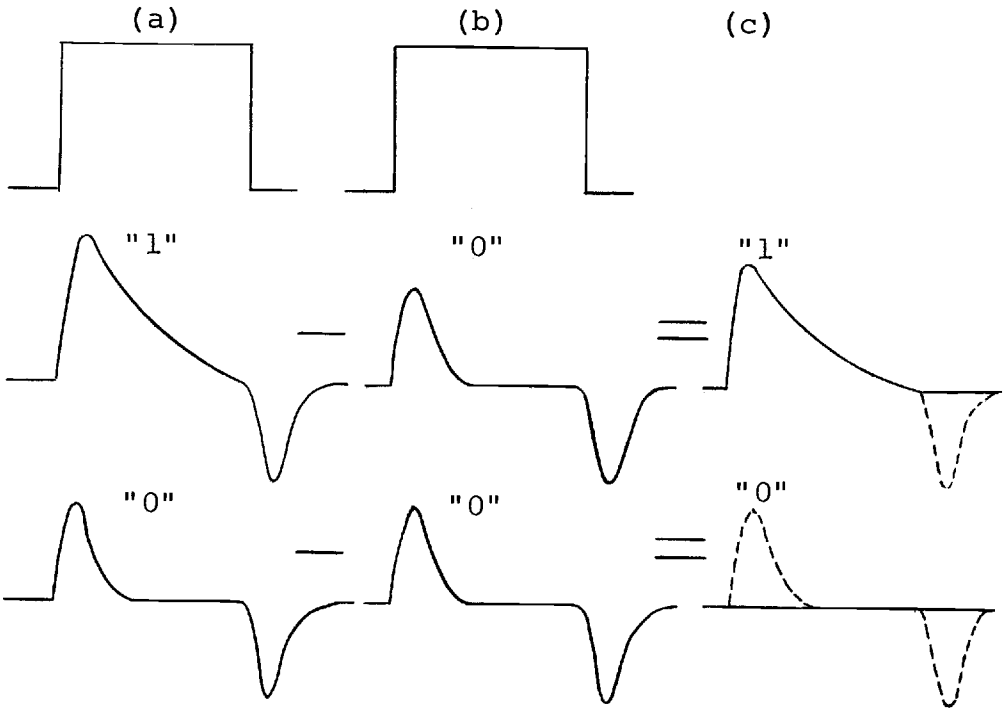

Figure 10. Principle of ideal compensation.

a) Read current pulse I_R, uncompensated "undisturbed 1", uV_1, and "undisturbed 0", uV_z, outputs.

b) Compensation current pulse I_c, and uncompensated "undisturbed 0", uV_z, outputs.

c) Compensated "undisturbed 1", cV_1, and "undisturbed 0", cV_z, outputs.

Suppose the storage cell is subjected to a read pulse, I_R, after a "1" was already written by a write pulse, I_w. An uncompensated "1" output, similar to the one in Figure 6(a), is induced in the sense winding. At the same time, the read command signal also activates the compensation driver, which delivers a compensation current pulse, I_c, to the compensation cell. Since the

state of the compensation cell is always at the "0" state, because of the absence of write pulse, an uncompensated "undisturbed 0" output similar to the one in Figure 6(b) is also induced in the sense wire. Because of the way the sense wire is threaded, these two sense-winding voltages with opposite polarities will subtract from each other. The difference between them is the compensated output voltage. The effect of this subtraction is shown in Figure 10(c). From the pictures in Figure 6, one can see that the compensated "undisturbed 1" output, cV_1, will have the "nonswitching" negative peak completely removed, the "tail" will be shortened and the peak amplitude reduced. Similarly, the compensated "undisturbed 0" output, cV_z, will have a perfect cancellation with no output voltage at all.

The above description of compensation is idealized, by assuming identical cells in a perfectly homogeneous material. In practice it was found not to be true. No matter how close the compensation was, there were always small "nonswitching" signals present in the sense-winding voltage.

The uncompensated outputs of Figure 6 were compensated, and the results are shown in Figure 11. The compensated outputs, cV_1 and cV_z, show a considerable reduction of "nonswitching" signals. The "nonswitching"

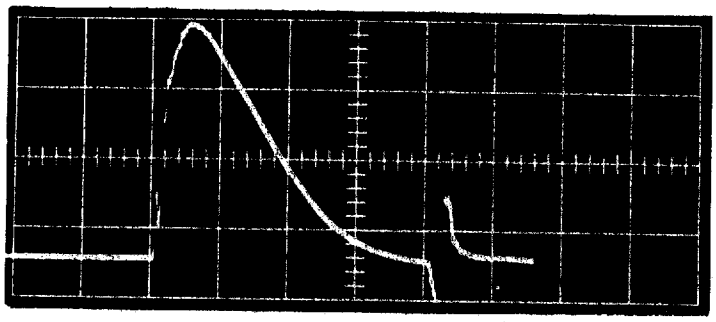

(a)

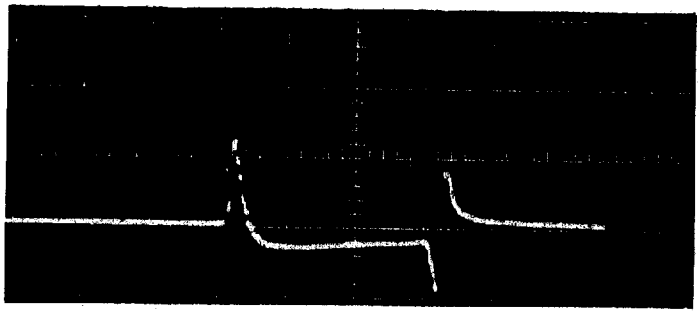

(b)

Scale: Horizontal = 0.5 microseconds per division.
Vertical = 5 millivolts per division.

Figure 11. Sense-winding voltages for the compensated, apertured Deltamax memory cell.

a) Compensated "undisturbed 1", cV_1.
b) Compensated "undisturbed 0", cV_z.

Write drive (N_dI_w) = 800 milliampere-turns
Read drive (N_dI_R) = 800 milliampere-turns
Compensation drive (N_dI_c) = 600 milliampere-turns
Write pulse width (t_d) = 1 microsecond
Read and compensation pulse width (t_d) = 2 microseconds
Pulse rise time (t_r) = 0.15 microsecond
Pulse fall time (t_f) = 0.1 microsecond
Frequency = 1 kilocycle

negative peak of Figure 6(a) was reduced from -28 millivolts to a plus and minus four millivolts, and the "nonswitching" signals of Figure 6(b) were reduced from 25 millivolts to about five millivolts. Note also that the cV_z amplitude at the peaking time, t_p, is about zero volt, giving a perfect discrimination between "1" and "0" outputs. The plus and minus "nonswitching" signals at the end of the cV_1 and cV_z are caused by the unequal storage time and fall time of the read and compensation pulses. The cV_1 is reduced from 35 millivolts to 17 millivolts. This reduction is expected, because of partial cancellation from the output of the compensation cell. The peaking time, t_p, is shifted to the right, thus increasing the t_p from 0.15 microsecond to 0.25 microsecond. The switching time, t_s, however, remained about the same.

Since the compensation itself has proved not suitable for improving the switching speed of memory cell, another scheme was added to increase the switching speed. It consists of removing the driving field soon after the peak of cV_1 by terminating the drive pulse. Figure 12 shows the cV_1 output waveforms for a read pulse width of one microsecond and 0.5 microsecond. The switching times obtained were about one microsecond and 0.5 microsecond respectively. By examining the pictures in Figure 12

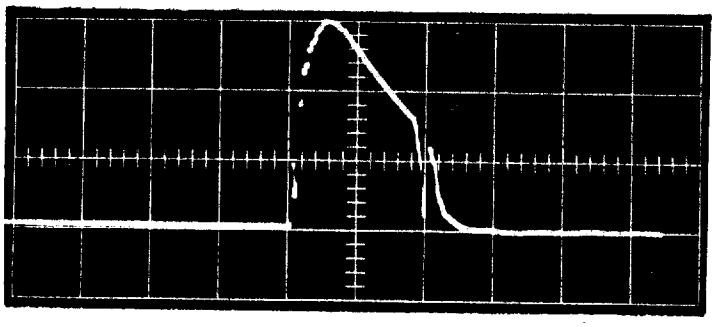

(a)

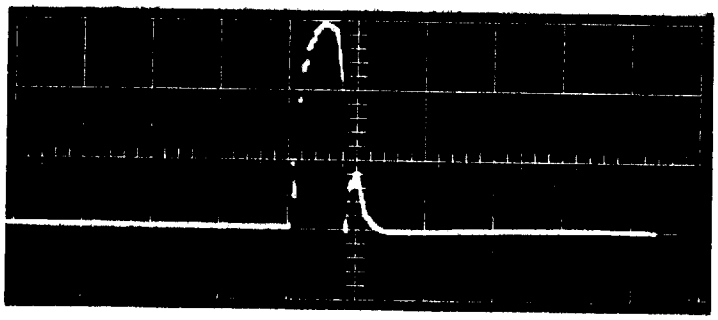

(b)

Scale: Horizontal = 0.5 microsecond per division.
Vertical = 5 millivolts per division.

Figure 12. Sense-winding voltages for the compensated, apertured Deltamax memory cell with reduced read and compensation drive pulse widths.

a) Compensated "undisturbed 1", cV_1, for drive pulse width of 1 microsecond.
b) Compensated "undisturbed 0", cV_z, for drive pulse width of 0.5 microsecond.

Write drive ($N_d I_w$) = 800 milliampere-turns
Read drive ($N_d I_R$) = 800 milliampere-turns
Compensation drive ($N_d I_c$) = 600 milliampere-turns
Write pulse width (t_d) = 1 microsecond
Pulse rise time (t_r) = 0.15 microsecond
Pulse fall time (t_f) = 0.1 microsecond
Frequency = 1 kilocycle

it can be seen that, as the pulse width was decreased, the "tail" was clipped. The bipolar "nonswitching" signals were elevated along the "tail" path and became partially hidden by cV_1 output. The peaking time remained the same, but the peak amplitude of cV_1 was slightly reduced by two millivolts.

To illustrate the speed improvement process shown in Figure 12, the penetration of flux reversal curve of Figure 7 was redrawn as shown in Figure 13, where the successive clipping of the "tail" for the responses shown in Figure 12 compared with that in Figure 11(a).

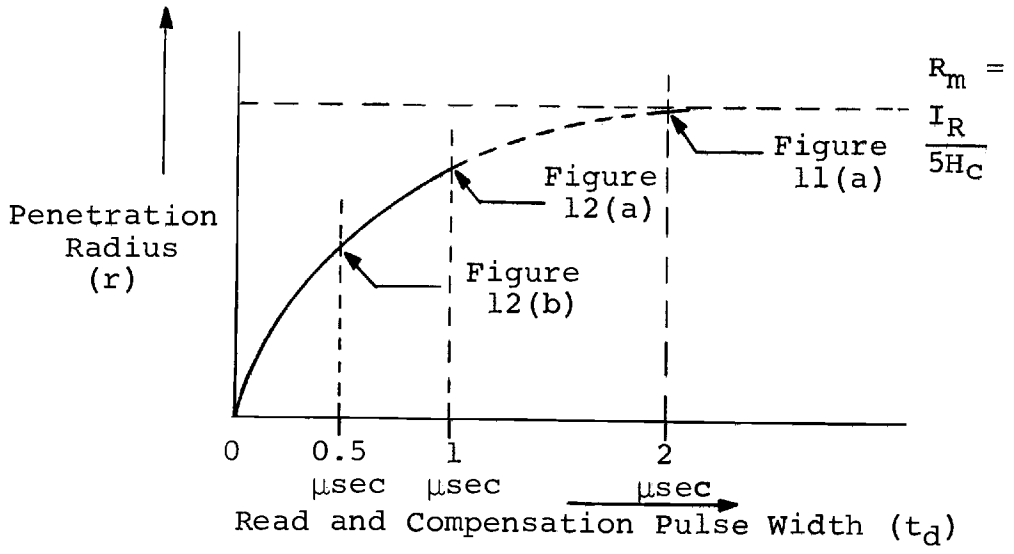

Figure 13. Principle of speed improvement.

7. Frequency Response of Compensated Deltamax Memory Cell

The word driver, as discussed in Appendix III, has its output current limited to 500 milliamperes, unless extra stages were added in parallel. Currents higher than 500 milliamperes were obtained safely by operating the word driver at a low duty cycle. Hence, the memory cell response so far obtained was operated at one kilocycle or less depending on the magnitude of the driving current. To investigate the response of memory cell at higher frequencies than one kilocycle, the drive currents were kept below 500 milliamperes. The pictures in Figure 14 show the high frequency responses of the compensated memory cell. Alternate write "1" and read "1" pattern was used. Note that the compensated "undisturbed 1" read outputs, cV_1, are preceded by the uncompensated "undisturbed 1" write outputs, uV_1.

There were no changes in the cV_1 and cV_z outputs as the frequency was increased from one kilocycle to 100 kilocycles. When the frequency was increased to 200 kilocycles, a decrease of two millivolts was observed for cV_1, while cV_z started to go negative. At frequencies above 200 kilocycles, cV_1 and cV_z started to deteriorate rapidly; almost a 50 percent decrease in cV_1 at 220 kilocycles, and a 60 percent decrease at

300 kilocycles.

The cV_z at 100 kilocycles show a nearly perfect compensation, except for the large positive and negative overshoot. At 200 and 220 kilocycles the cV_z went negative, which will help to improve the discrimination between "1"s and "0"s, because the cV_z negative voltage can be detected and rejected very easily by the sense amplifier. The cV_z at 300 kilocycles, however, is not desirable because of large negative and positive peaks, which are particularly harmful to the transistors in the sense amplifier.

Further examination shows that the memory cell could not be operated at its full speed. Figure 14 shows a cycle time, t_c, of four microseconds which means it could be operated at a maximum frequency of 250 kilocycles without any deterioration of its output signals. The actual cause for this poor frequency response was not determined. However, the possible factors which might contribute to this poor frequency response, such as the large eddy current loss due to high conductivity of Deltamax material, the switching loss due to self heating of the memory cell at high frequency, the memory cell geometry and its associated electronic circuitry, should be considered.

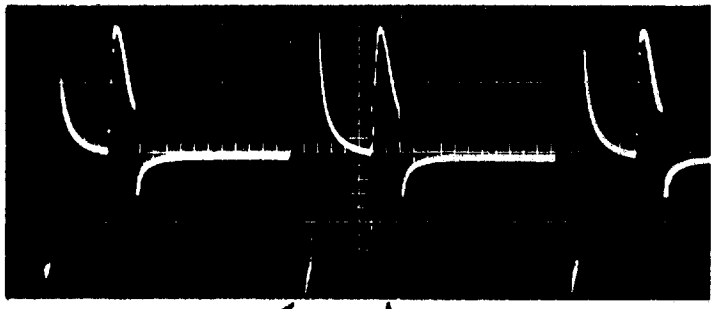

Uncompensated
write "1"

Compensated
read "undisturbed 1",
cV_1

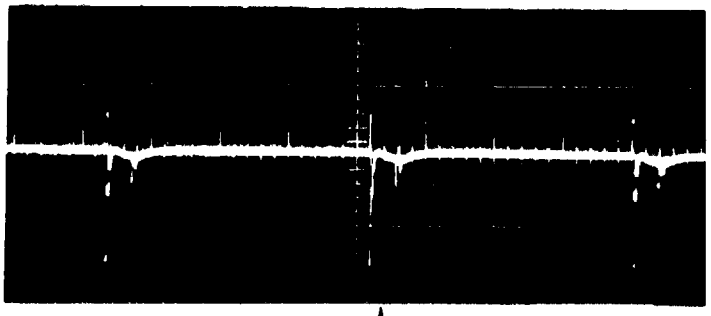

Compensated
read "undisturbed 0",
cV_z

Frequency = 100 kilocycles

Scale: Horizontal = 2.5 microseconds per division
Vertical = 5 millivolts per division

Figure 14. Frequency response of the compensated, apertured Deltamax memory cell.

Read drive (N_dI_R) = 450 milliampere-turns
Write drive (N_dI_w) = 500 milliampere-turns
Compensation drive (N_dI_c) = 400 milliampere-turns
All pulse width (t_d) = 1 microsecond
Pulse rise time (t_r) = 0.15 microsecond
Pulse fall time (t_f) = 0.1 microsecond

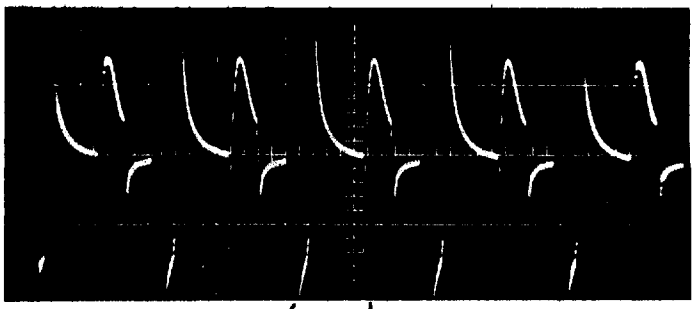

Uncompensated
write "1"

Compensated
read "undisturbed 1",
cV_1

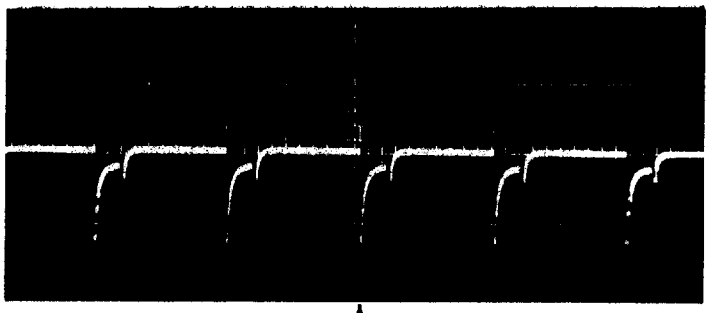

Compensated
read "undisturbed 0",
cV_z

Frequency = 200 kilocycles

Scale: Horizontal = 2.5 microseconds per division
Vertical = 5 millivolts per division

Figure 14. (Continued)

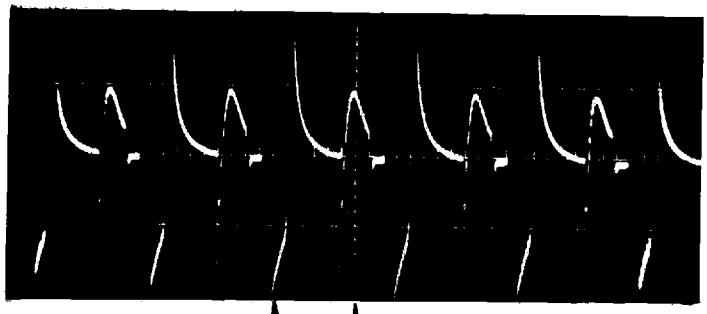

Uncompensated
write "1"

Compensated
read "undisturbed 1",
cV_1

Compensated
read "undisturbed 0",
cV_z

Frequency = 220 kilocycles

Scale: Horizontal = 2.5 microseconds per division
Vertical = 5 millivolts per division

Figure 14. (Continued)

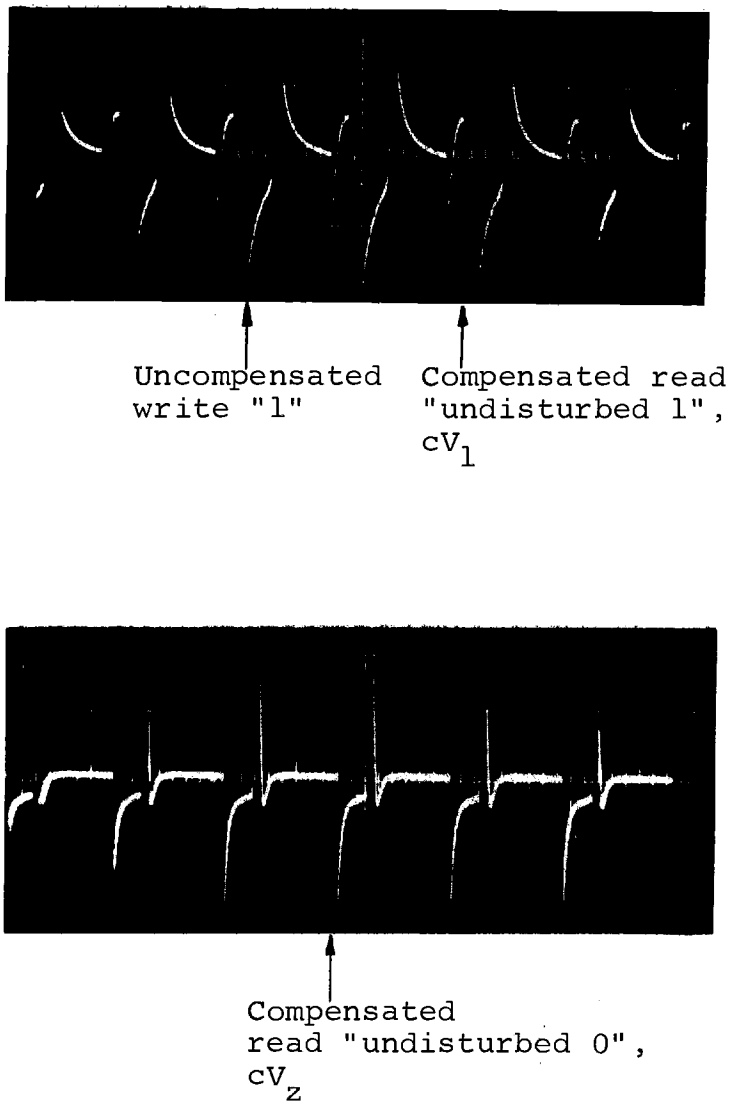

Frequency = 300 kilocycles

Scale: Horizontal = 2 microseconds per division
Vertical = 5 millivolts per division

Figure 14. (Continued)

8. Operating Range of the Compensated Deltamax Memory Cell

Several response curves have been plotted for the compensated memory cell.

The curves shown in Figures 15 (Table 3), 16 (Table 4) and 17 (Table 5) show the effects of the compensation drive current, I_c, on the response of the compensated memory cell, for fixed read currents of one ampere, 800 milliamperes, and 500 milliamperes respectively. The write current was fixed at 800 milliamperes, enough to completely saturate the memory cell after each read operation. The system was operated at one kilocycle. It may be noted from these graphs that the compensated "undisturbed 1", cV_1, and compensated "undisturbed 0", cV_Z, decreases as the compensation drive current, I_c, increases. This is expected, since the progressive increase of the compensation cell's output, due to increase of I_c, diminished gradually the output from the storage cell in the process of compensation. This can be seen from the negative values of cV_Z, that come from overcompensation at high I_c. The dashed line at the cV_Z curve shows the transition period from positive value to negative value, where cV_Z has a bipolar waveform.

The switching time, t_s, shows no appreciable

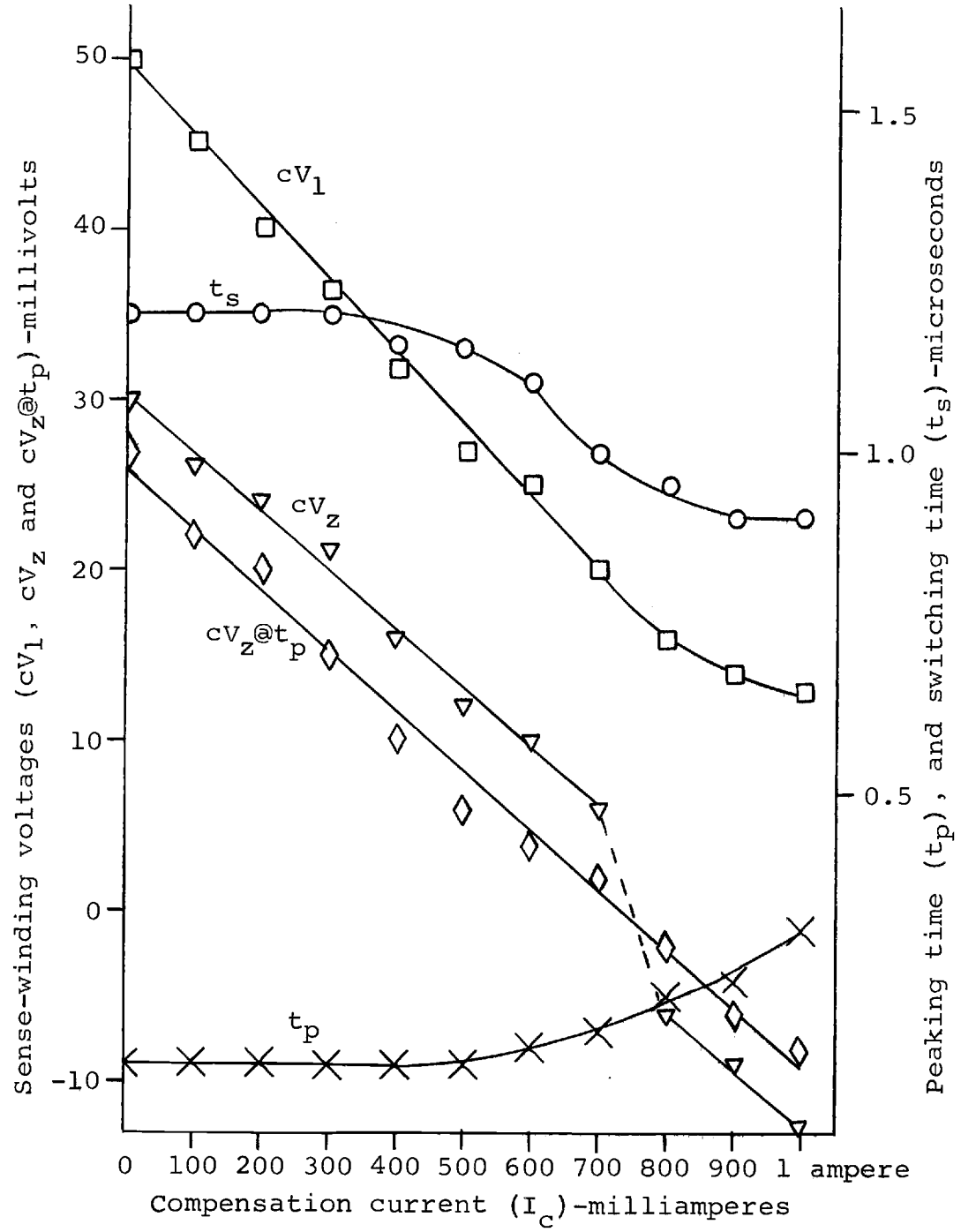

Figure 15. Typical characteristics of compensated, apertured Deltamax memory cell with a read current pulse of one ampere.

(See Table III, Appendix VI for test conditions)

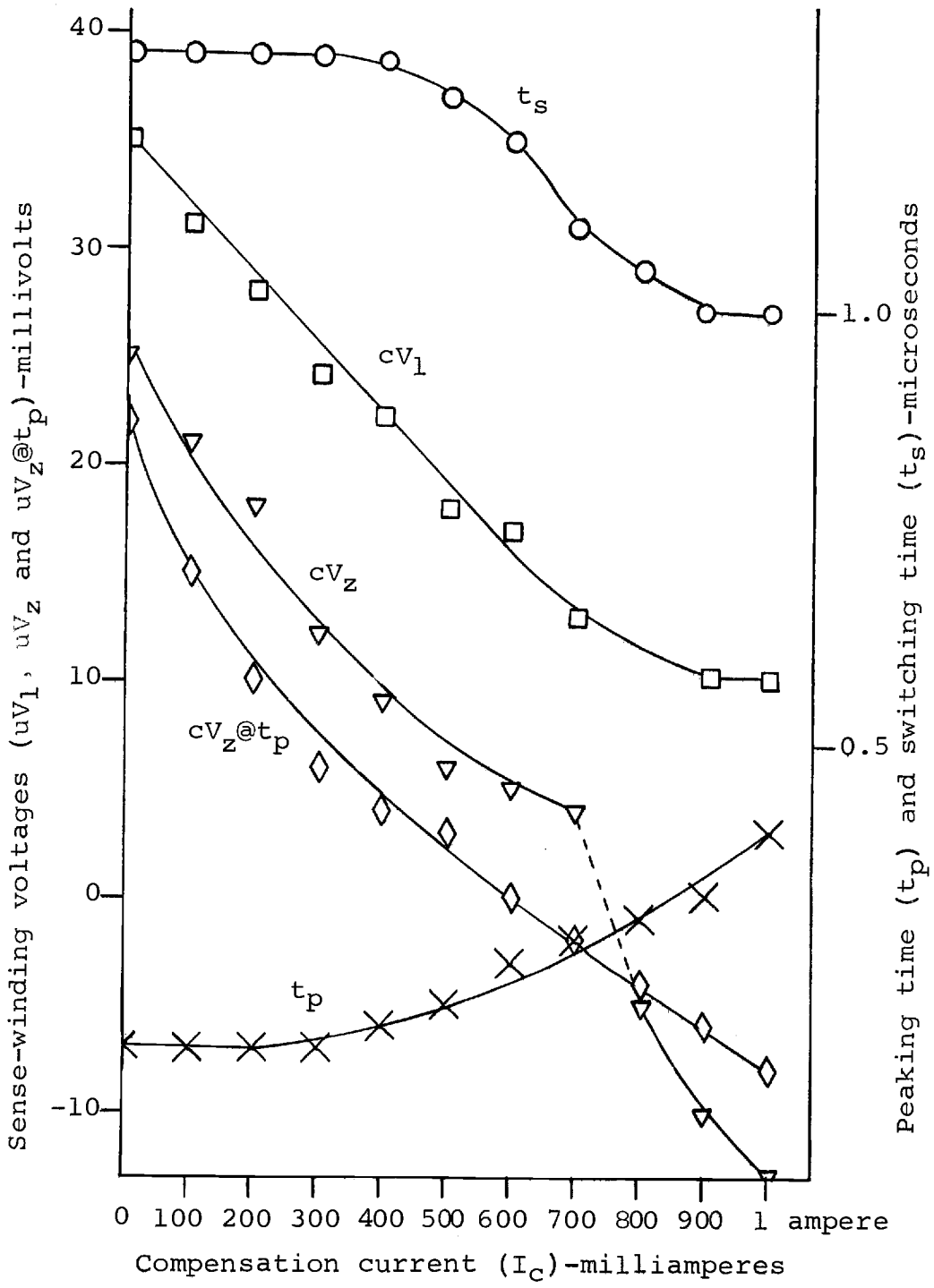

Figure 16. Typical characteristics for the compensated, apertured Deltamax memory cell with a read current pulse of 800 milliamperes. (See Table IV, Appendix VI, for test conditions)

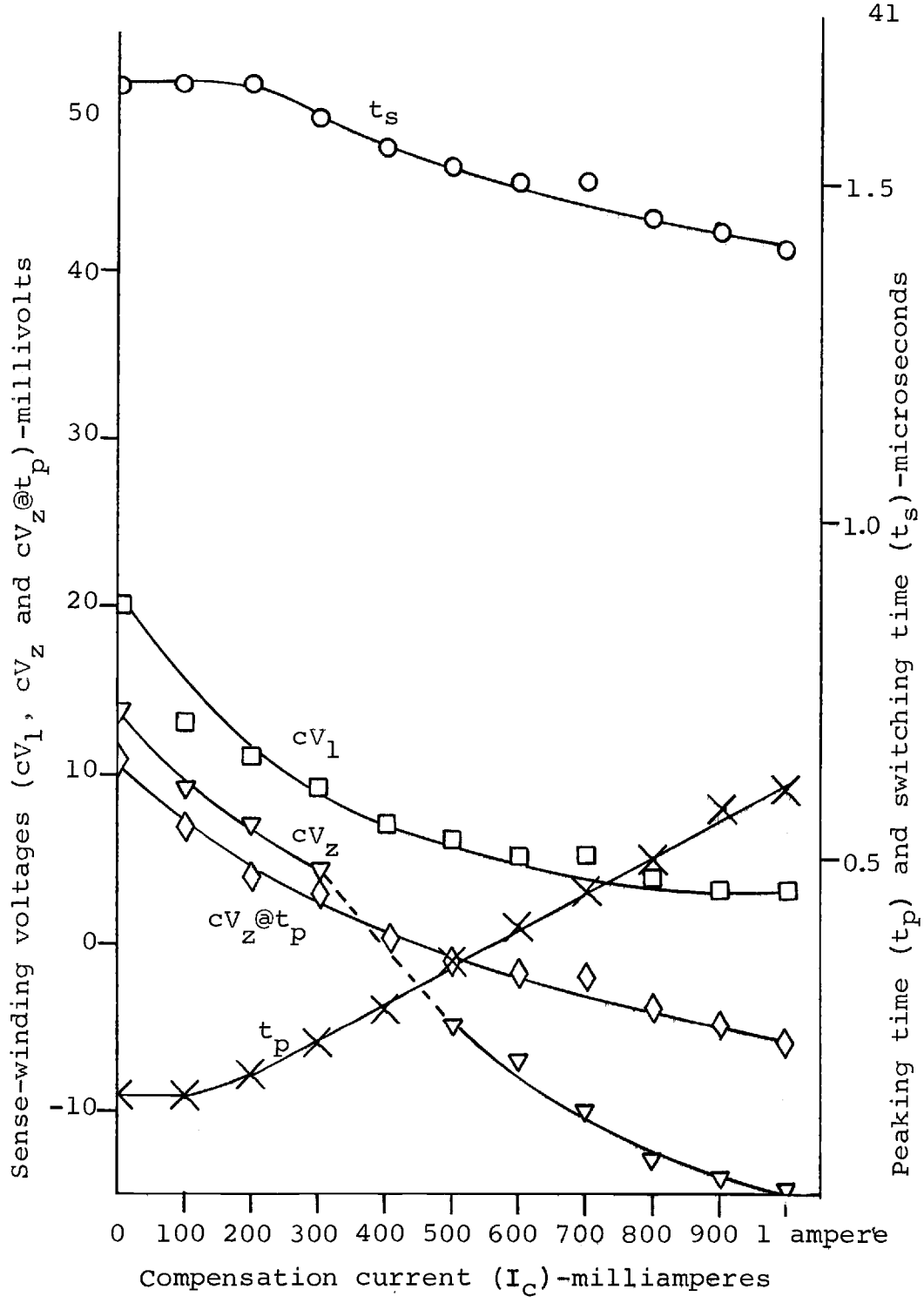

Figure 17. Typical characteristics of compensated, apertured Deltamax memory cell with a read current pulse of 500 milliamperes.

(See Table V, Appendix VI for test conditions)

improvement over that of uncompensated response. This indicates that the adjustment of drive pulse width discussed previously should be used.

The peaking time, t_p, appears to be constant until a certain value of I_c is applied; after that it starts to increase. For lower read current, I_R, it shows the t_p starts to increase at a lower value of I_c and has a higher rate of increase. This significant shift of t_p results in a proportional shift of cV_z @ t_p. This is shown in the graphs, where the curves for cV_z @ t_p intercept that of cV_z, instead of following the cV_z curve as it does in Figure 8, where t_p is fairly constant.

The best operating points obtained from these graphs are shown in Table I.

Table I. Best Operating Points for Compensated Deltamax Memory Cell.

	Operating Points			Compensated Memory Cell Response				
Figure	I_w	I_R	I_c	cV_1	cV_z	cV_z@t_p	t_p	t_s
15	800ma	1 amp	600ma	25mv	10mv	4mv	0.13 μsec	1.1 μsec
16	800ma	800ma	600ma	17mv	5mv	0mv	0.25 μsec	1.2 μsec
17	800ma	500ma	400ma	7mv	-	0mv	0.27 μsec	1.55 μsec

The optimum operating ranges of I_c, for each value of the read current shown above, are centered at 600

milliamperes, 600 milliamperes and 400 milliamperes respectively with plus or minus 100 milliamperes from each side.

The curves shown in Figures 18 (Table 6) and 19 (Table 7) show the effects of write current, I_w, and write pulse width, t_d, on the response of the compensated memory cell. The similarity of these curves indicates that equal effects were obtained from I_w and t_d.

Examining the curves, we can see that the switching time, t_s, and the compensated "undisturbed 1", cV_1, changed considerably, while the peaking time, t_p, and the compensated "undisturbed 0", cV_z, remained constant. For write current above 800 milliamperes, and write pulse width above 0.9 microsecond, the values of cV_1 and t_s are constant, and below these values the cV_1 and t_s start to decrease very rapidly. These changes can be explained as follows: if the write "1" has a lower drive current, I_w, or narrower pulse width, t_d, than that of the read "1" drive, the effective penetration of flux reversal due to the larger read drive magnetomotive force will be stopped by the lesser penetration of the opposite polarity flux reversal of the smaller write drive magnetomotive force. Hence the resultant cV_1 will be small, due to small amount of flux change, and the switching time will also be small because of the excess read drive.

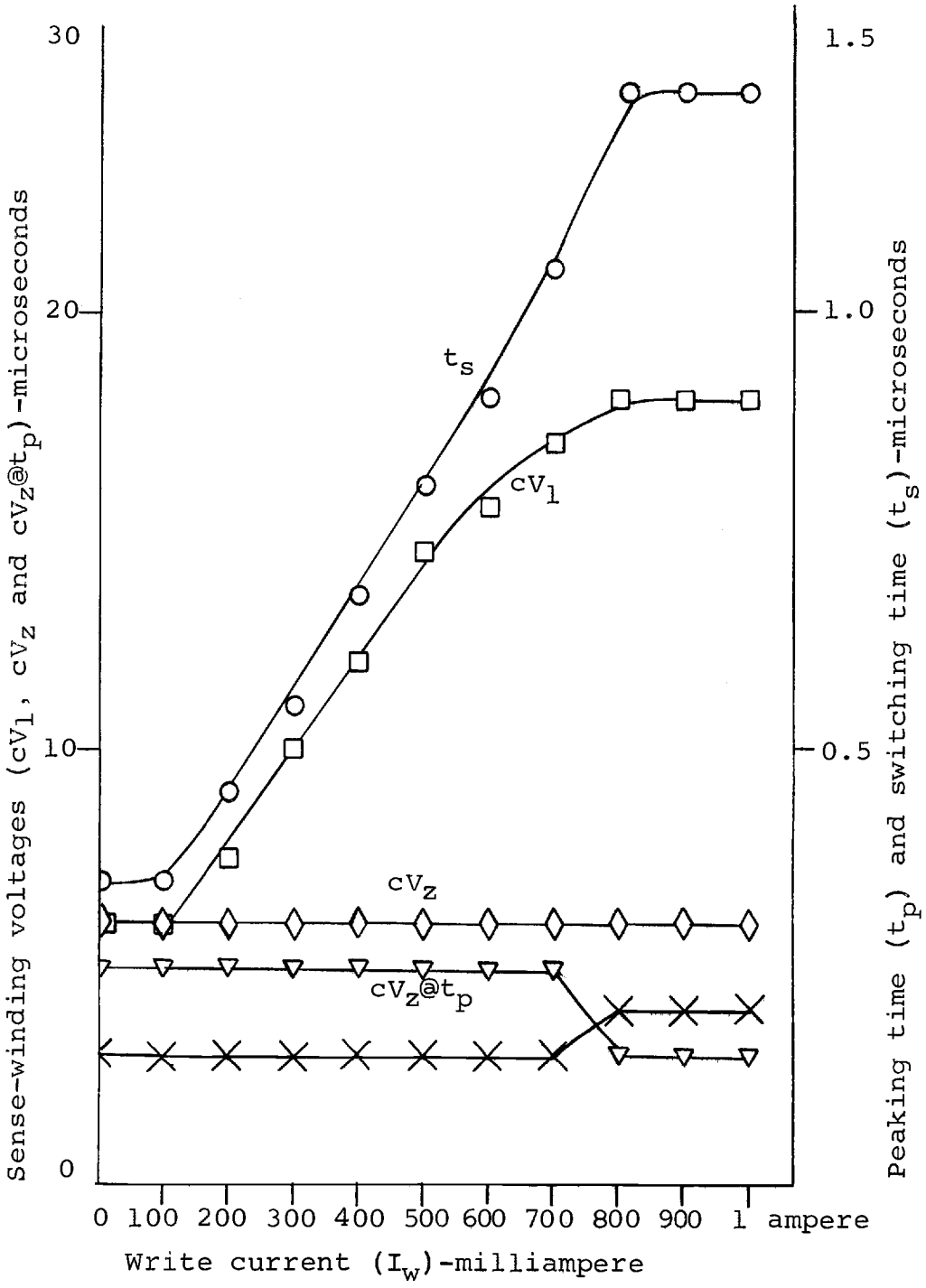

Figure 18. Variation of typical characteristics for the compensated, apertured Deltamax memory cell with write current, (I_w).

(See Table VI, Appendix VI, for test conditions)

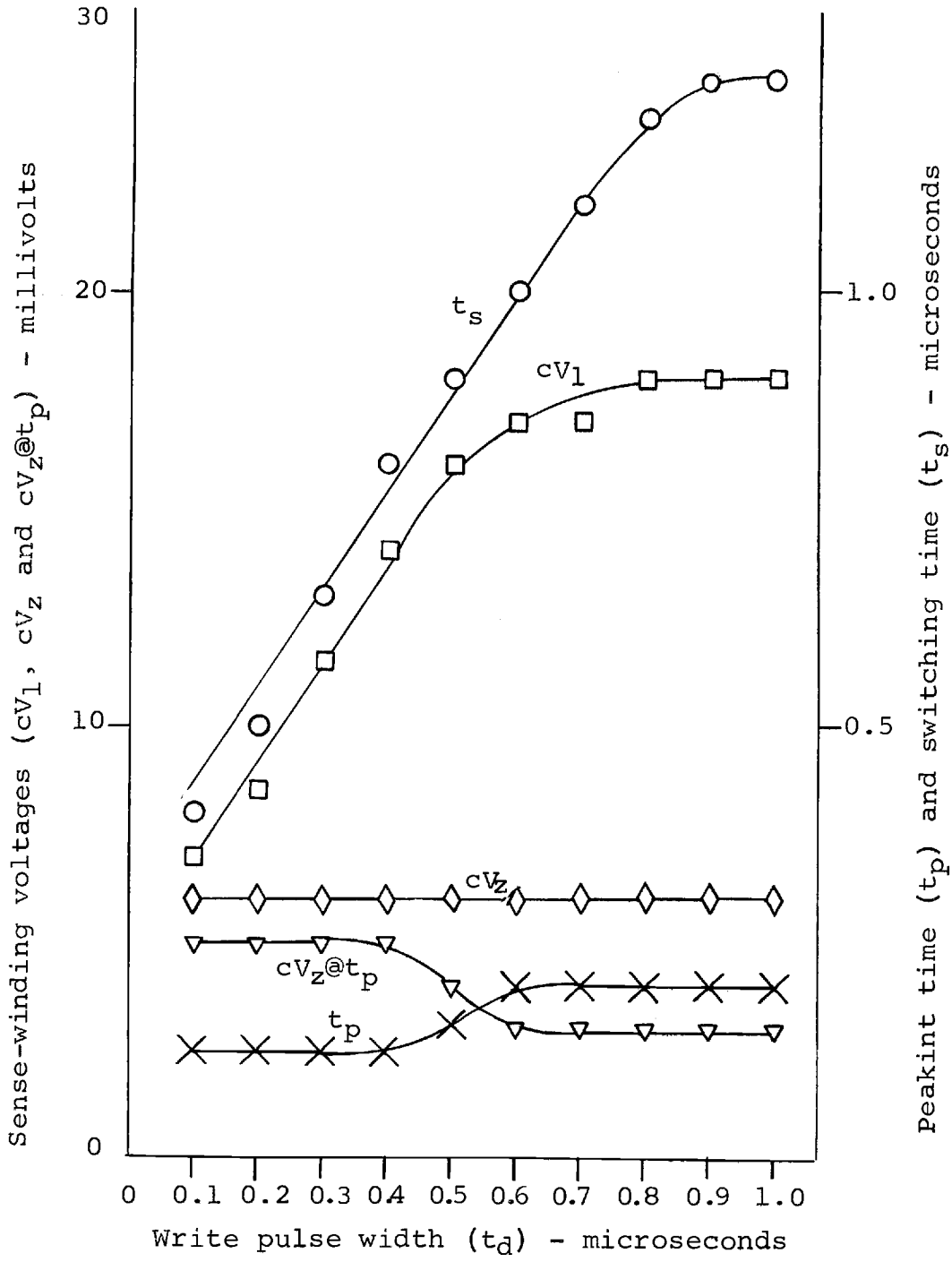

Figure 19. Variation of the typical characteristics for the compensated, apertured Deltamax memory cell with write pulse width (t_d).

(See Table VII, Appendix VI, for test conditions)

If the write "1" penetration is made equal to or deeper than that of the read, the effective penetration of the read drive will be allowed to reach its full value. As the result of this, cV_1 and t_s will increase toward a constant value.

It should be noted that Figures 18 and 19 show the importance of selecting a proper write current magnitude and pulse width. It should also be noted that a compromise should be made between a faster switching time and a larger sense-winding voltage, when selecting a particular write drive.

9. Effects of Temperature on the Compensated Deltamax Memory Cell

Figure 20 (Table 8) shows the effect of temperature on the memory cell. The memory cell was placed in a temperature controlled chamber, Delta design Model 1060L, and the temperature test was run from -75°F to 425°F. Dry ice was used as a coolant in the temperature chamber for low temperature test. Each point on the graph was measured at the specific temperatures indicated. The memory cell was held at each temperature for approximately five minutes. To drive the memory cell, a read current, I_R, of 800 milliamperes, a write current, I_W, of 800 milliamperes, and a compensation current, I_C, of 600 milliamperes were used. The same temperature test

was run for the RCA-226M1 ferrite core; its response is shown in Figure 21 (Table 9).

Figures 20 and 21 show the "undisturbed 1" outputs for the core, uV_1, and for the compensated memory cell, cV_1, start to increase as the temperature rises above the room temperature, 75°F. The same effect is observed for the "undisturbed 0" outputs, uV_z and cV_z. When the temperature reaches 250°F the uV_1 starts to decrease rapidly and reaches zero at 425°F. The value of uV_z starts to decrease at 350°F and reaches zero at 425°F. However, the temperature response curves for compensated memory cell shown in Figure 20 indicate no such changes at 250°F and 425°F. The values for cV_1 and cV_z appear to be continuing to increase in the positive direction.

To analyze these facts, the change of magnetic properties of ferrite and Deltamax with the change of temperature was considered. As the temperature of ferrite core and memory cell increases, both the saturation flux, B_s, and coercive force, H_c, decrease, finally reaching zero at the curie point. The curie point of most square-loop ferrite lies in the region 150°-300°C (302°-572°F). From Figure 21, the curie point obtained for the ferrite core is 425°F. The curie point for Deltamax is not known, but it can be seen from Figure 32 (Appendix IV), that the curie point for Deltamax is much higher than

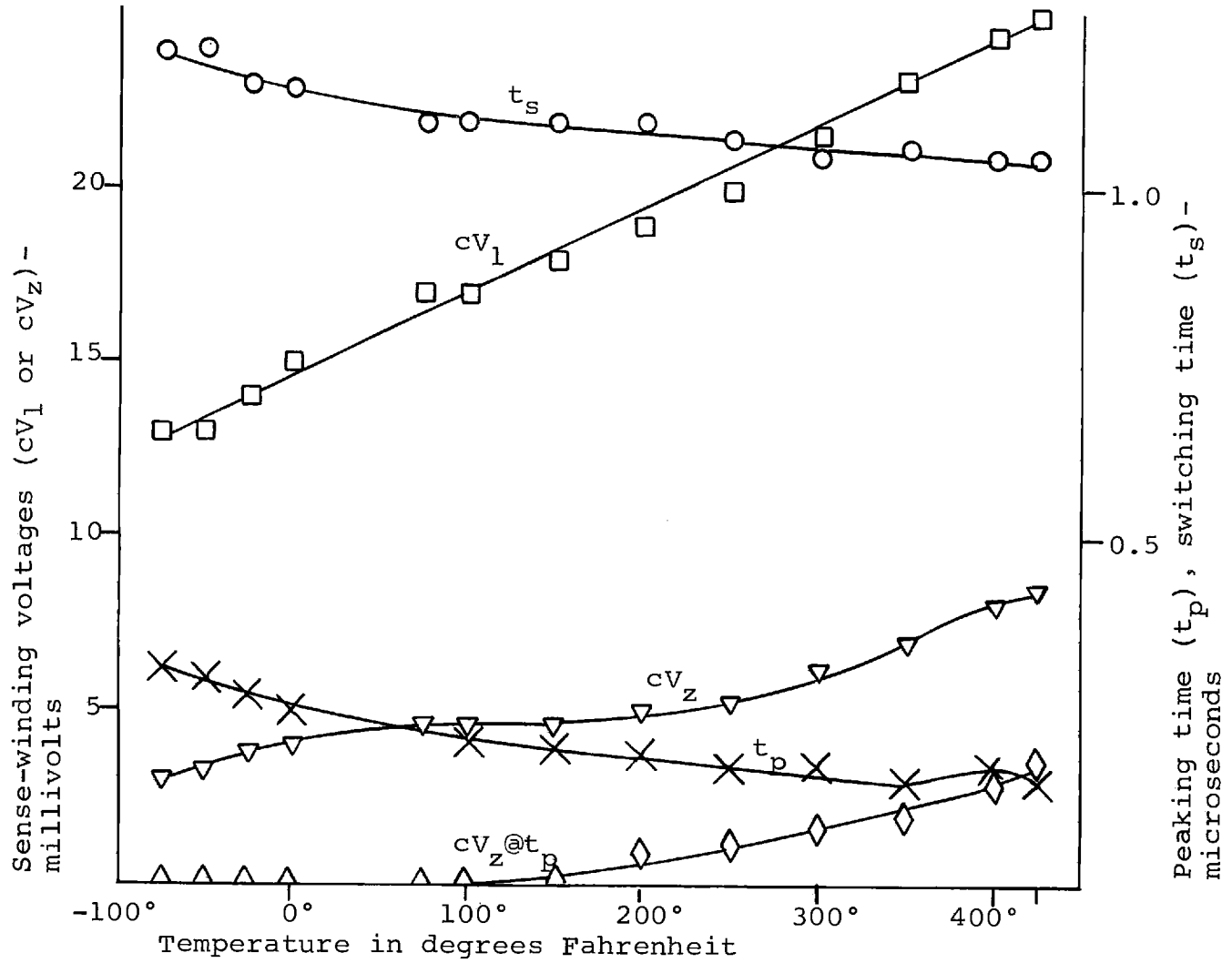

Figure 20. Temperature effect on the response of the compensated, apertured Deltamax memory cell. (See Table VIII, Appendix VI)

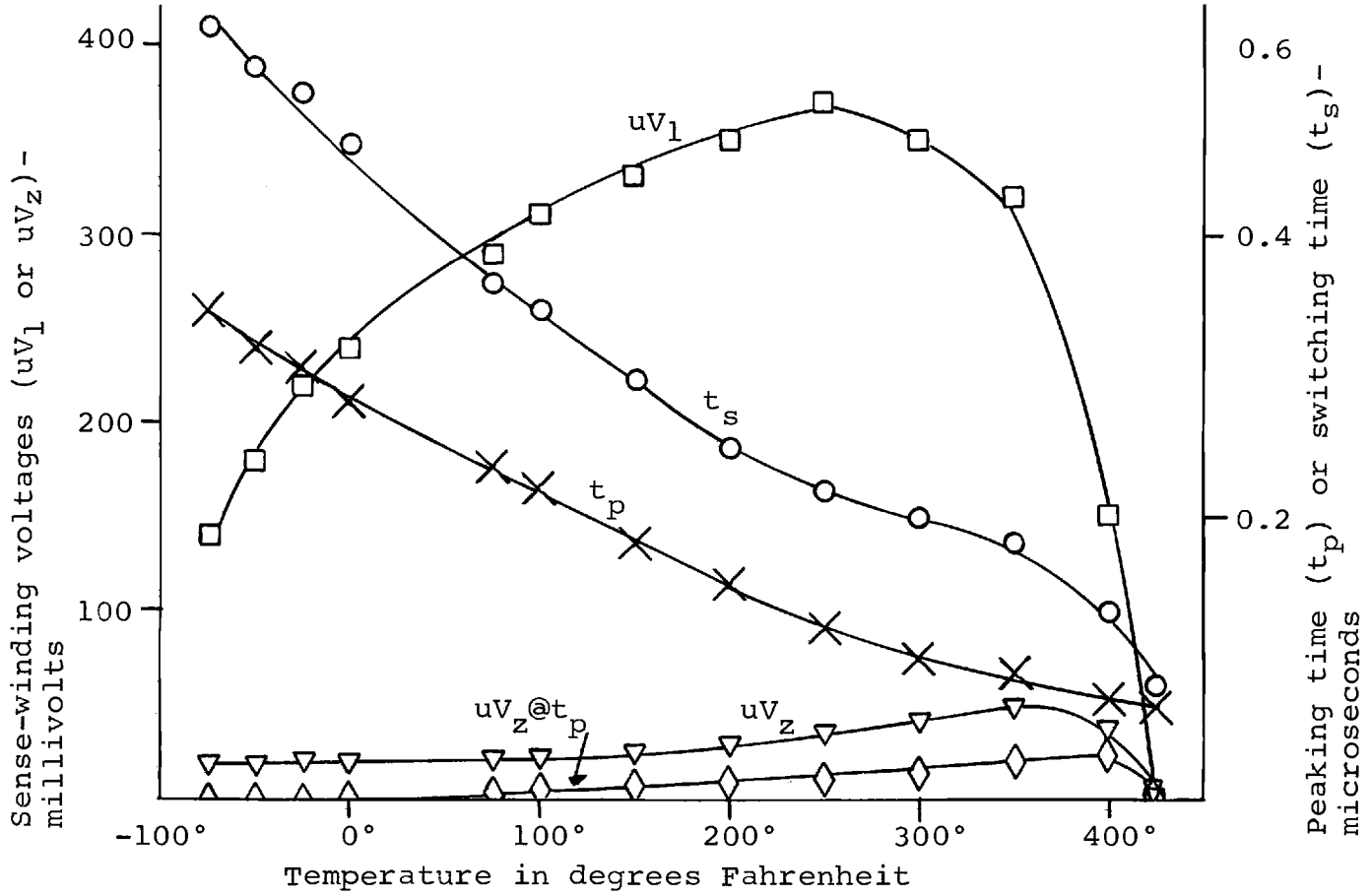

Figure 21. Temperature effect on the RCA Type 226M1 ferrite core.

(See Table IX , Appendix VI for test conditions)

that for ferrite core. Hence a much higher temperature is necessary in order to reduce the outputs of the memory cell to zero. As the temperature starts to increase from the room temperature, the value of H_s starts to decrease. The drive current, being the same, overdrives the ferrite core and the memory cell. This excessive drive current reduces the switching time and consequently increases the sense output amplitude. For the ferrite core, the increase of output due to excessive drive predominates over the effect of saturation flux reduction from 75°F to 250°F. For temperatures higher than 250°F the reduction of saturation flux becomes the predominant factor, causing the output to decrease rapidly to zero as the curie point is reached. The switching time and the peaking time, however, still continue to decrease due to the excessive drive. In the case of the memory cell, a much higher temperature is needed to cause any significant reduction of saturation flux so as to become the predominant factor in reducing the output of the memory cell. Figure 20 shows that the temperature at which this would occur is at least higher than 425°F.

For temperatures below room temperature, the value of saturation flux decreases and the value of coercive force increases for both ferrite core and memory cell.

As the saturation flux decreases, the amount of flux change decreases, and so does the output voltage. As the coercive force increases, the drive current, being the same, underdrives the core and the memory cell. This results in a further output reduction and increase in switching time and peaking time.

Figures 20 and 21 clearly show that the operation of memory cell is possible over a wider temperature range than that of ferrite core. It was concluded from this work that the apertured Deltamax memory cell definitely has better temperature characteristics than the commonly used ferrite cores.

It should be emphasized that the values shown in Figures 20 and 21 were recorded with the core and memory cell held at the temperatures indicated for only five minutes. It is not known whether repeated temperature cycles, or maintaining the ferrite core and memory cell at high or low temperatures for a long period of time, would alter the magnetic properties of both the ferrite core and memory cell permanently after allowing them to return to room temperature.

CONCLUSION

The operation of the apertured Deltamax memory cell has been discussed, analyzed and documented in some detail.

The principle of operation of the memory cell was described by comparison with the operation of ferrite cores. Typical response of the memory cell, namely the long "tail" and large "nonswitching" signals were identified and analyzed. It was found that the compensation method should be employed to improve the discrimination between "1"s and "0"s to an acceptable level. It was also shown that the only effective way to reduce the switching time of the memory cell is to remove the driving field soon after the peaking time, by reducing the drive pulse width. However, it was discovered later that we could not obtain the full benefit of this reduced switching time because the operation speed of the memory cell is limited by some factors still not determined.

Several memory cell response curves under different drive conditions were obtained. From these curves the proper drive requirements for the memory cell were found. Large drive requirements, poor discrimination ability and poor frequency response of the memory cell compared with that of the ferrite core, makes the memory cell an unfavorable choice. However, its cost reduction potential

still makes this type of memory worthy of consideration. In the temperature test the memory cell was much better than ferrite core.

The etching process used to make the memory cell has not been thoroughly developed. The memory cell used, however imperfect, served its purpose for this thesis. The data obtained from the experimental memory cell may not be as good as that which could be obtained from a perfectly finished sample, but it did show the feasibility of the apertured Deltamax memory cell as a batch fabricated, and inexpensive memory device.

BIBLIOGRAPHY

1. Arnold Engineering Company. Properties of ...Deltamax, 4-79 Mo-permalloy, and Supermalloy. Rev. ed. Marengo, Illinois, 1951. 26 p. (Bulletin Tc-101)

2. Eastman Kodak Company. Kodak photosensitive resists for industry. Rochester, N.Y., 1962. 56 p. (Kodak Industrial Data Book P-7)

3. Galt, J. K. Motion of individual domain walls in a nickel-iron ferrite. Bell System Technical Journal 33:1023-1054. 1954.

4. Gillot, D. H. and J. F. Calvert. Eddy current loss in saturated solid magnetic plates, rods, and conductors. Institute of Electrical and Electronics Engineers Transactions on Magnetics 1(2):126-137. 1965.

5. Goodenough, J. B. The influence of chemistry on B/H loop shape coercivity and flux reversal time in ferrites. Proceedings of the Institute of Electrical Engineers (London) 104B (Suppl. no. 7): 400-410. 1957.

6. Kraus, John D. Electromagnetics. New York, McGraw-Hill Book Company, Inc., 1953. 604 p.

7. Leifer, M. S. Pulse-width temperature-controlled megacycle core memory. Institute of Electrical and Electronics Engineers Transactions on Communication and Electronics 83:281-294. 1964.

8. Millman, Jacob and Herbert Taub. Pulse, digital, and switching waveforms. New York, McGraw-Hill Book Company, Inc., 1965. 958 p.

9. Murakami, K. An experimental study of flux pre-setting-resetting characteristics of magnetic cores with rectangular hysteresis loop. Institute of Electrical and Electronics Engineers Transactions on Magnetics 1(2):91-95. 1965.

10. Quartly, C. J. Square-loop ferrite circuitry. Englewood Cliffs, N.J., Prentice-Hall, Inc., 1962. 166 p.

11. Rajchman, J. A. Ferrite apertured plate for random access memory. Proceedings of the Institute of Radio Engineers 45:325-334. 1957.

12. Riddler, D. S. and R. Grimmond. The magnetic cell: A new circuit element. Proceedings of the Institute of Electrical Engineers (London) 104B (Suppl. no. 7):445-456. 1957.

13. Shahbender, R. et al. Microaperture high-speed ferrite memory. Radio Corporation of America Review 23(4):539-566. 1962.

14. Shahbender, R. et al. Laminated ferrite memory. Radio Corporation of America Review 24(4):705-729. 1963.

APPENDICES

APPENDIX I

Type II Element

The type II element consists of a hole in a stack of magnetic tape. The principle of operation of type II element is the same as that of Deltamax memory cell described in Section 2, page 6.

The magnetic tape used in this investigation is the type used in computer memory. It consists of a Mylar base of about 1.5 mils in thickness and a magnetic coating, which may range from 0.3 to 0.7 mil in thickness. The magnetic coating is made up of finely divided iron oxide particles embedded in a binder. The coercivity for this magnetic coating is expected to be in the range from 180 to 270 oersteds. To overcome this high coercivity, the increased read and write drive current pulses of eight amperes shown in Figure 30 were used. Figure 22 shows the system diagram of the type II element. The paper stack with about the same dimensions as the tape was used to cancel the effect of the tape's Mylar base material, which is nonmagnetic. Figure 23 shows a top view of the type II element with the sense and drive windings.

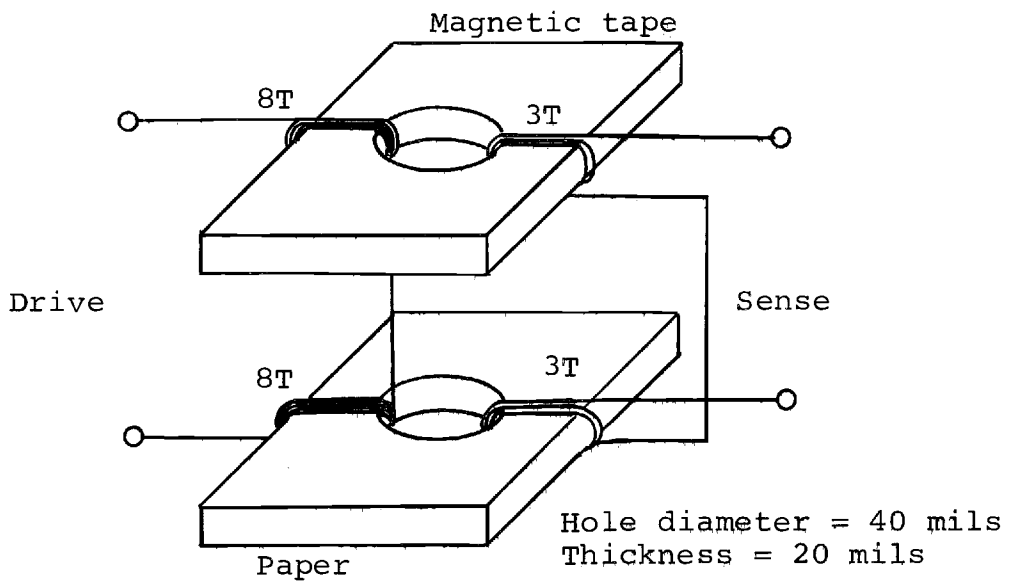

Figure 22. Type II element system diagram.

The magnetomotive force applied was about

$$F = N_d \times I = 8 \text{ turns} \times 8 \text{ amperes} = 64 \text{ ampere-turns}.$$

The sense-winding outputs, however, showed no trace of possible discrimination between the "1"s and "0"s. The maximum output was about three millivolts. Flux reversal patterns were observed from the individual tape cell under a magnetic tape viewer. The flux reversal patterns were distributed heavily along the drive winding and lightly along the sense winding. No flux reversal pattern linking both the drive and sense windings was observed, which indicates that the sense-winding output signals are not generated from the resultant change of flux with magnetic coating, but rather from the coupling noises.

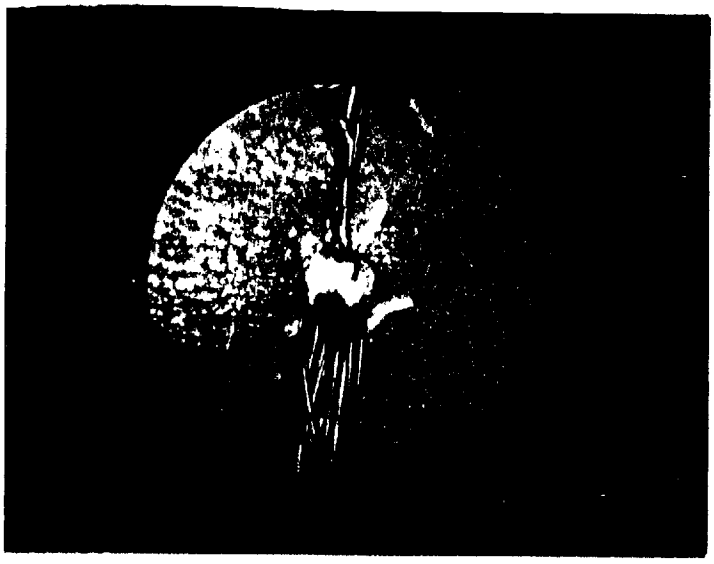

Magnification: X10

Figure 23. Top view of the Type II element with the drive and sense windings.

Factors which impeded any further investigation of the type II element at the present time are: (1) drive current requirements; (2) small volume of the magnetic coating material; (3) slow rise time of the amplified bipolar drive pulse; (4) the poor response of the magnetic coating on the tape to this type of excitation.

APPENDIX II

Type III Element

The type III element consists of two orthogonal wires, an x-directed wire and a y-directed wire. The crossover point between the x and y wires is embedded in a cylindrical block of magnetic material. The word current (read-write) is applied to the x-winding, and the y-winding is used for both digit current and sense output.

The experimental type III element structure is shown in Figure 24.

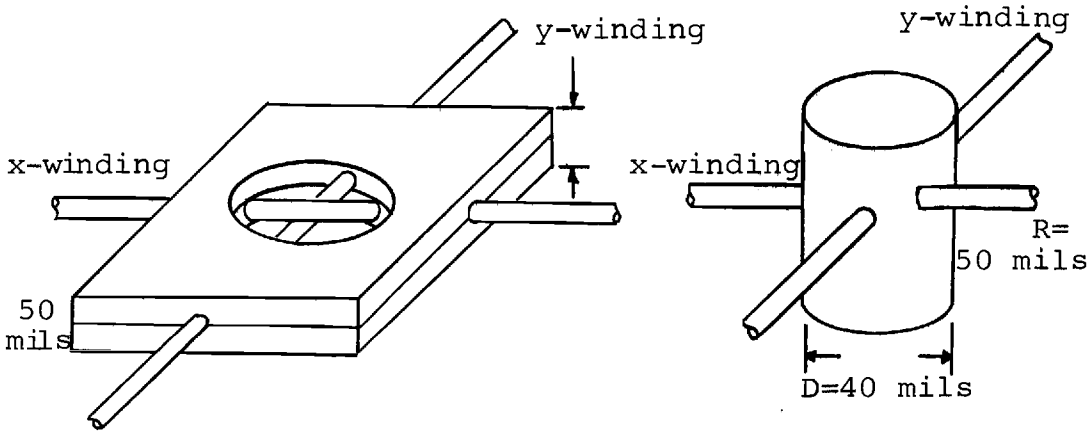

(a) (b)

Figure 24. Structure of type III element.

a) Perforated plastic sheets with the x and y windings.
b) Resultant pre-wired core.

Two plastic sheets, each 25 mils thick with a 40 mil hole, were used, and the x and y windings were sandwiched between them with the crossover at the center of the 40 mil hole as shown in Figure 24(a). The magnetic material, consisting of a mixture of iron oxide powder and epoxy binder, was packed into the hole. The mixture was air dried. The resultant pre-wired core in the form of a cylinder, with the dimensions 40 mils in diameter and 50 mils in height, is shown in Figure 24(b).

Operation of the type III element can be visualized with the aid of the vector diagram shown in Figure 25.

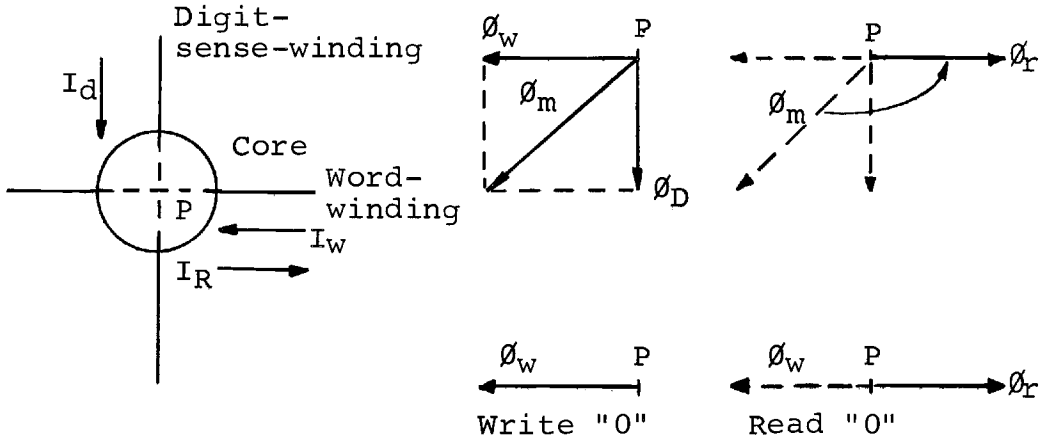

Figure 25. Flux vector diagram of type III element.

The magnitude of the vector is proportional to the flux switched by the drive current. The direction of the vector, by the right-hand rule, is in the direction of the current establishing the flux. To write a "1", a

digit pulse is applied to the digit wire in time coincidence with a write pulse. The flux switched by the word-write current, $\emptyset_w$, and the flux switched by the digit current, $\emptyset_D$, will switch a component of flux mutual to both the word and digit windings, $\emptyset_m$, at the crossover point, P, as shown in Figure 25. Upon the application of a read pulse, the mutual flux, $\emptyset_m$, reverses to the position, $\emptyset_r$, and induces a sense-winding voltage in the digit winding which is also the sense winding. To write a "0", no digit pulse is applied. Hence no mutual flux, $\emptyset_m$, is switched. Upon the application of a read pulse, the flux, $\emptyset_w$, reverses to the position, $\emptyset_r$, along the word wire that does not link the digit-sense wire because they are orthogonal to each other. Therefore, no sense-winding output voltage is induced.

The type III element was constructed according to the dimensions shown in Figure 24. A top view of the type III element before and after deposition of magnetic material is shown in Figure 26.

The system, however, did not work as was predicted in Figure 25, because the iron oxide powder has a high coercivity and increases further with the addition of the epoxy binder. Since only a single turn for the drive winding is allowed for this type of configuration,

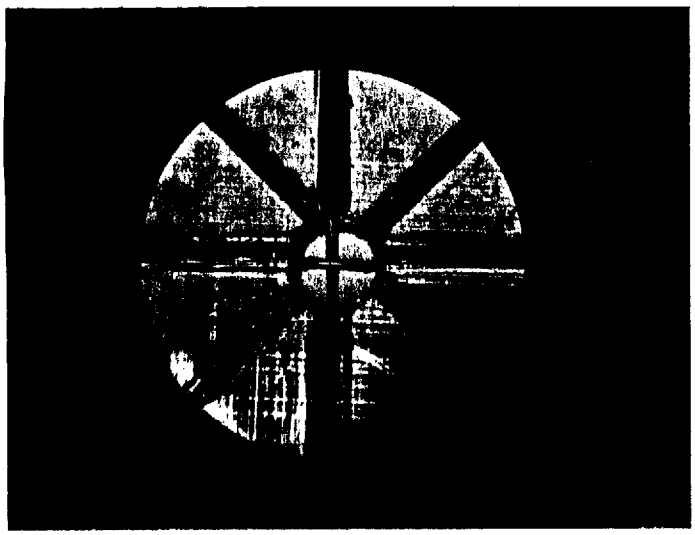

(a)

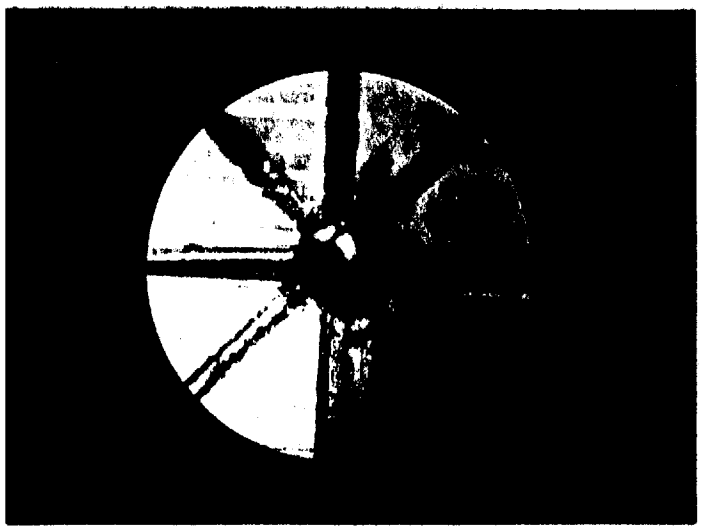

(b)

Magnification: X10

Figure 26. Top view of the Type III element.

a) Before deposition of magnetic powder, showing the word drive and digit-sense wires.
b) After deposition of magnetic powder.

the magnetomotive force in ampere-turn is insufficient to switch the core. Ferrite cores were crushed and used in place of iron oxide powder, but still no positive results were obtained. It should also be noted that the mixture of iron oxide powder with epoxy binder is very thick, it contains air inclusions which may cause a poor bonding around the crossover point, P, and at the same time increases the coercivity of the mixture.

A liquid slurry of a low coercive ferrite powder and appropriate organic binders would be the ideal mixture for this type of memory device.

APPENDIX III

Word-Driver Circuit

The function of the word-driver circuit was to supply a positive read current or negative write current.

The bipolar currents were obtained by using the bridge circuit shown in Figure 27. The word-driver consists of write and read switches, constant write and read current sources and sinks; it is driven by two pulse generators which generate read and write signals.

When a read signal is generated, it energizes point R which turns on transistors Q_1, Q_2 and the constant read current source, Q_3. This permits a constant read current pulse to flow in the core line from left to right. Similarly, when a write pulse is produced, the transistors Q_4, Q_5 and the write constant current source, Q_6 are turned on, and a constant write current pulse flows in the core line from right to left.

The basic constant current source operates as follows: the 2N3638 (Q_1) transistor is turned on by the read signal, causing point b to be at or near ground potential. Because of the voltage division between R_1 and R_2, a potential V_{BB} will appear between the base of transistor Q_3 and point a. A current will therefore flow in the emitter resistance R_e which is equal to

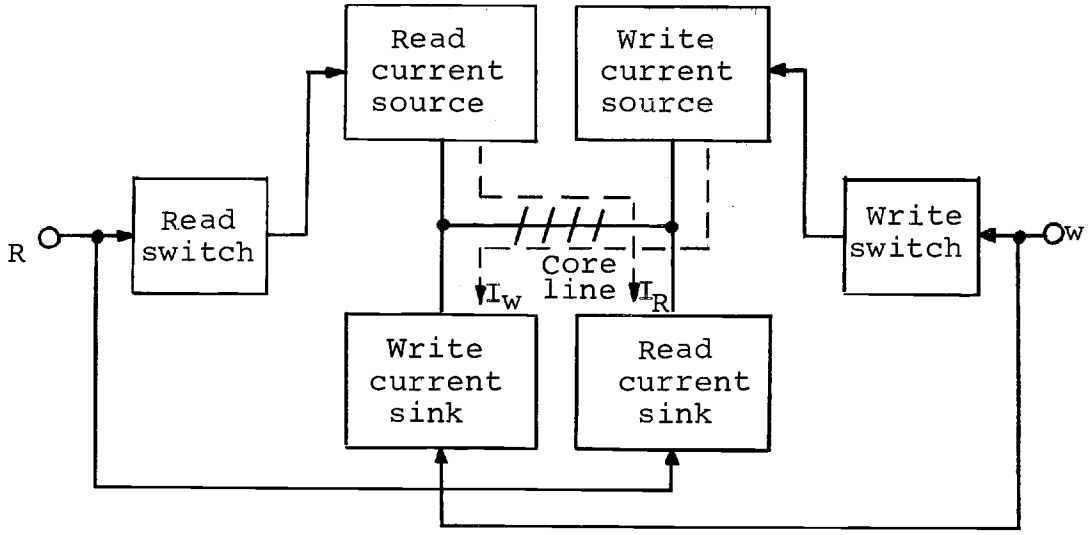

(a)

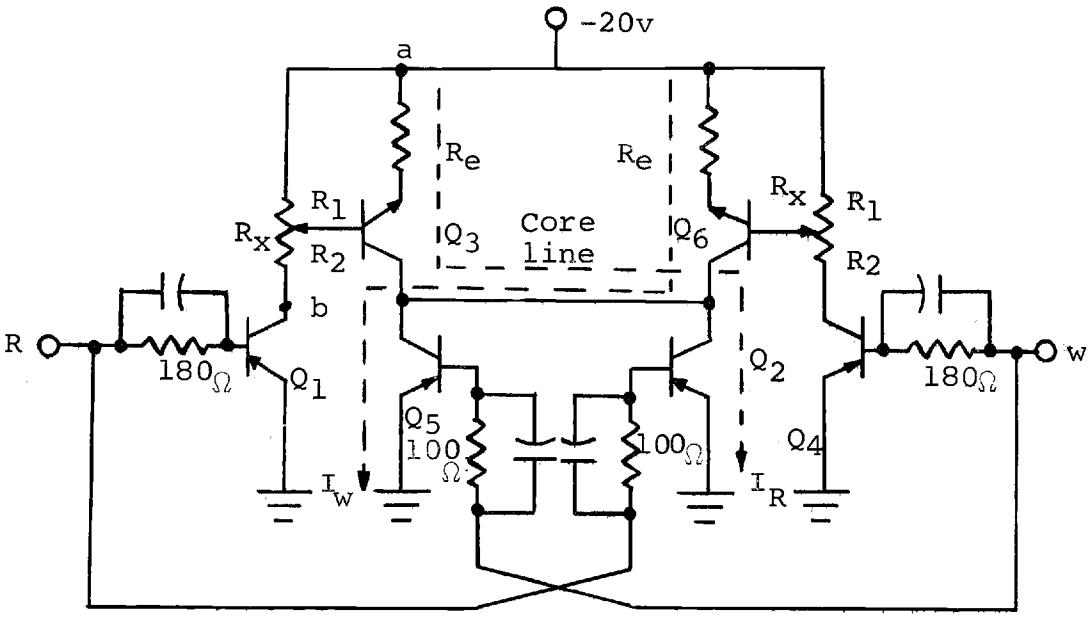

(b)

All PNP transistors are 2N3638 $R_e = 15\Omega$
All NPN transistors are 2N3643 $R_x = 500\Omega$
All capacitors are 150 picofarads

Figure 27. Word-driver.

(a) Block diagram
(b) Circuit diagram

$$I_e = \frac{V_{BB} - V_{BE}}{R_e}$$

where V_{BE} is the drop between the base and emitter of Q_3. The current in the collector will therefore be αI_e, where α is usually in the range of 0.97-0.99. The constant read current and write current magnitude can be varied continuously by adjusting the potentiometers, R_x, where V_{BB} can be increased or decreased as the center tap of the potentiometer is moved downward or upward respectively. The ability of fine adjustment of the constant read and write currents make the measurements more convenient.

The 2N3643 and 2N3638 are NPN and PNP silicon planar epitaxial transistors. They were selected because they are designed for digital applications at current levels up to 500 milliamperes. The high gain-bandwidth product, f_T, at high current, makes it an excellent unit for line driving and magnetic memory applications.

To obtain higher driving currents than 500 milliamperes, identical current source and sink are paralleled at points a and b in order to share the extra current. For the sake of circuit simplicity, a constant bipolar output current of one ampere or more was safely obtained by operating the driver at a low duty cycle without adding extra transistors.

Figure 28 is an oscillogram of the read-write command signal pulses from the pulse generators, and Figure 29 shows the constant bipolar drive current pulses from the word-driver.

A further increase in the output current can be obtained by inserting a current step-up transformer in the word-driver output. The output transformer had a 12:1 turns ratio. Figure 30 is an oscillogram of the increased bipolar driving current of eight amperes in each direction. This increase in the driving current is necessary for driving the type II element as discussed in Appendix I.

It should be noted that the current gain of eight amperes shown in Figure 30 was obtained at the price of increasing the rise time. The increase of the rise time is caused by the leakage inductance and shunt capacitance of the pulse transformer, which increase with the large step-up ratio used in the pulse transformer. The response of the pulse transformer during the top of the pulse is tilted downward, because the iron core was driven into saturation. The response of the pulse transformer beyond the pulse width, $t > t_d$, is an exponential decay with the same time constant as that of the top of the pulse.

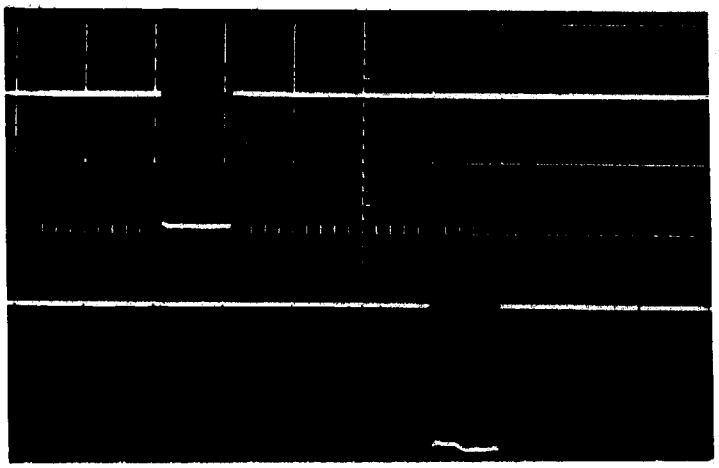

Scale: Horizontal = 2 microseconds per division
Vertical = 5 volts per division

Figure 28. Read and write command signals.

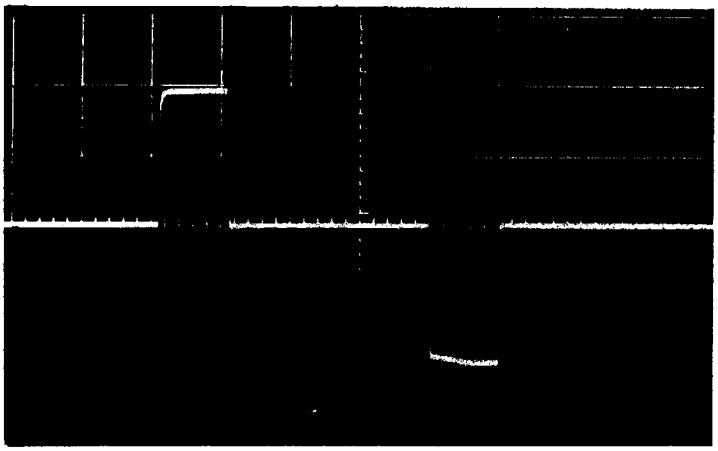

Scale: Horizontal = 2 microseconds per division
Vertical = 500 milliamperes per division

Figure 29. Read and write drive current pulses.

Frequency = 1 kilocycle

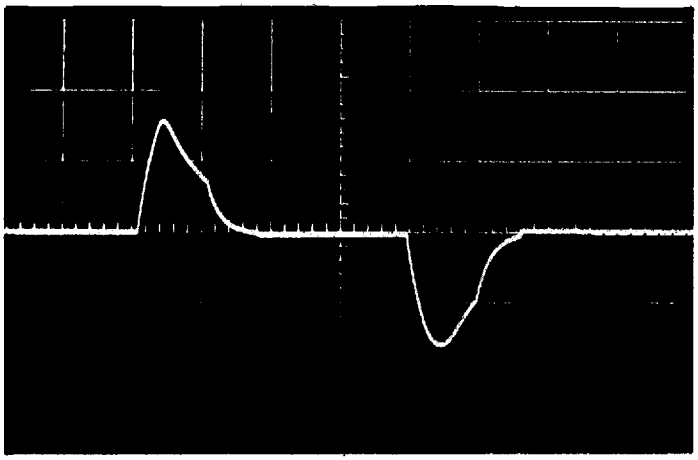

Scale: Horizontal = 2 microseconds per division
Vertical = 5 amperes per division

Figure 30. Increased read and write drive current pulses.

Frequency = 1 kilocycle

APPENDIX IV

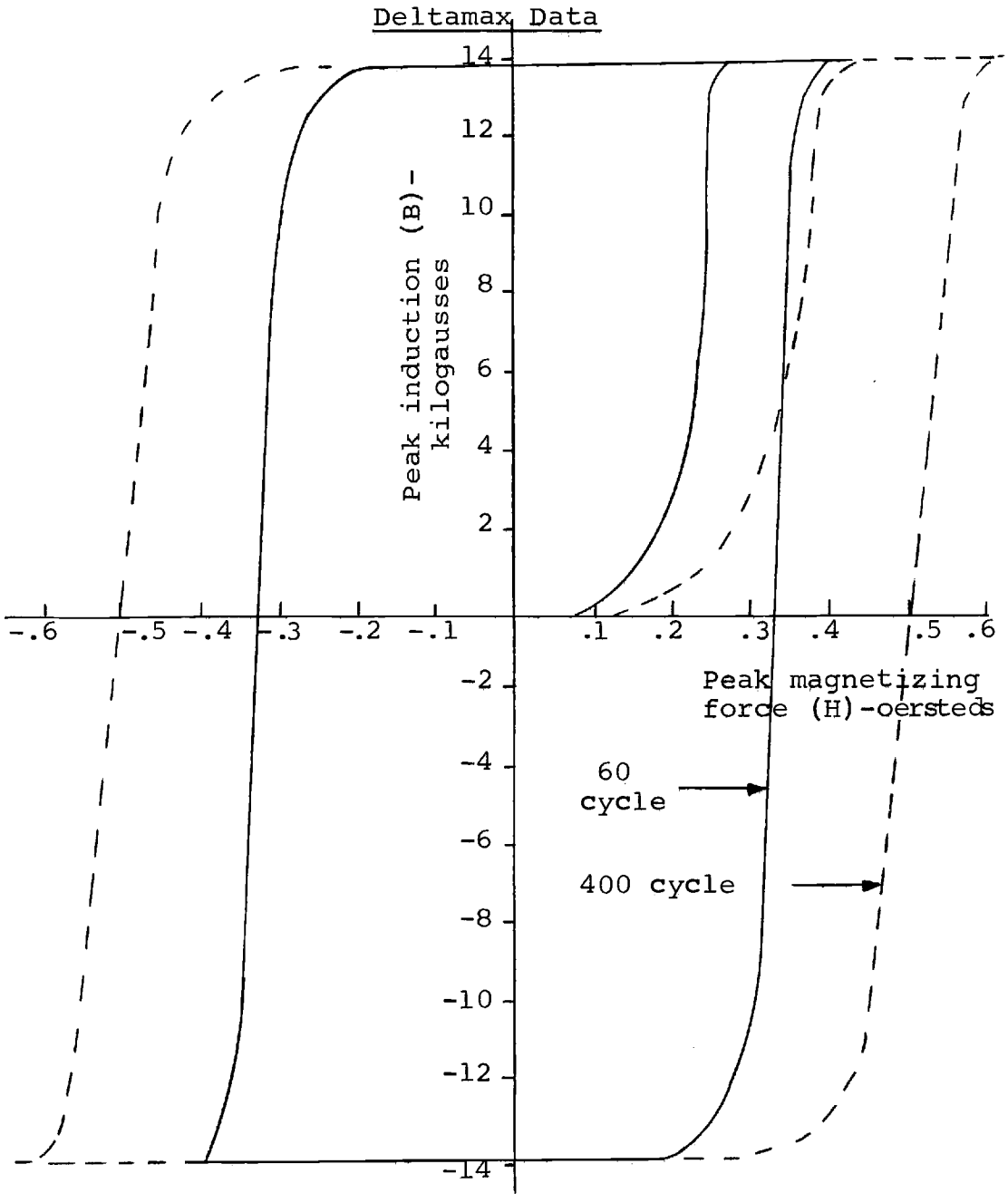

Figure 31. Dynamic magnetization loops of Deltamax.

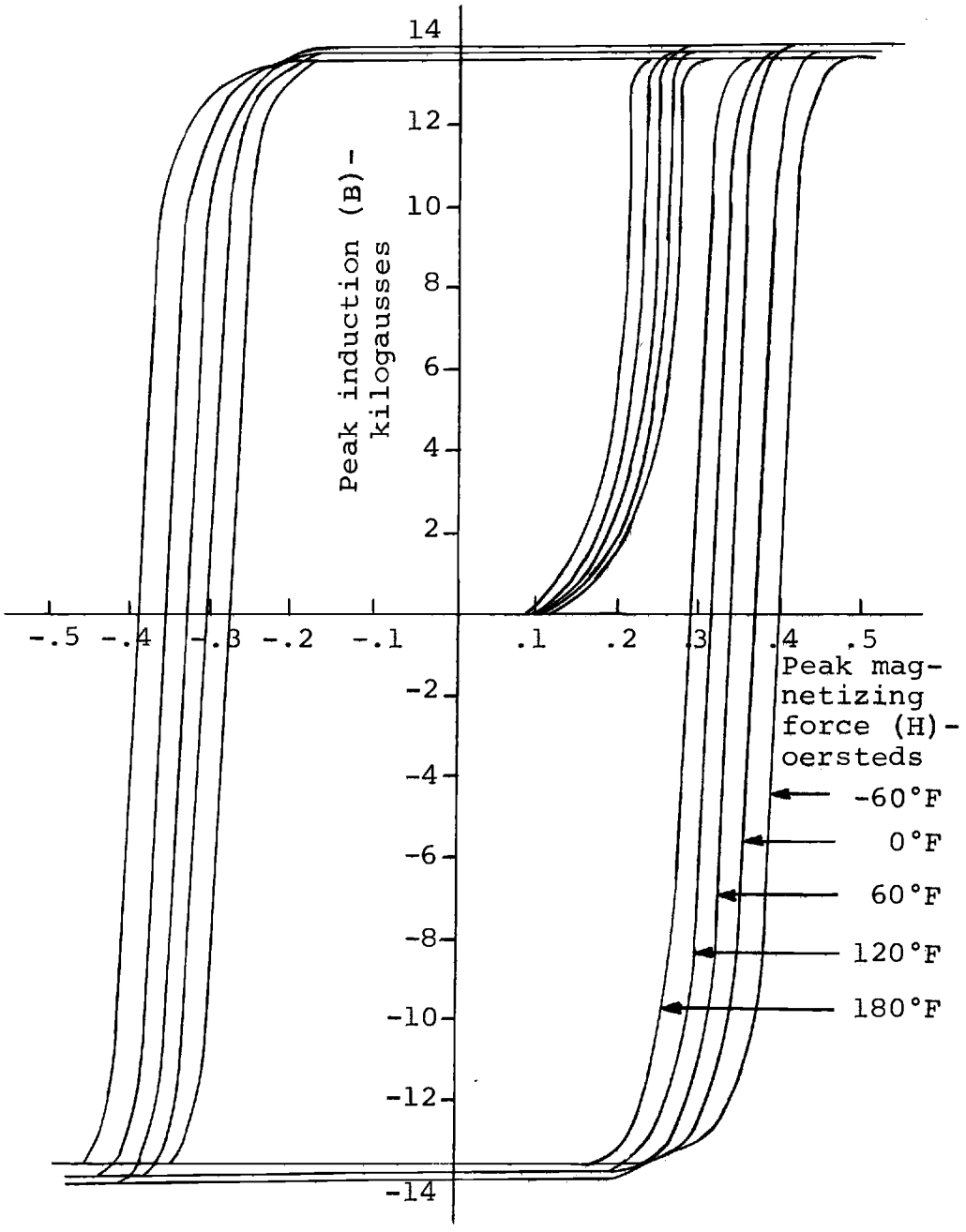

Figure 32. Effect of temperature on the dynamic magnetization loop of Deltamax at 60 cycles A.C.

APPENDIX V

Preparation of Etch Resistant Patterns on Deltamax Tape Using Kodak Thin Film Resist

Introduction

The process of preparing an etch resistant pattern for semiconductor work is described in general in a publication by Eastman Kodak Company (2).

Following is a description of a method used in etching holes through a thin tape of Deltamax as part of a study in an experimental memory device.

Operation

The basic procedures of photolithographic techniques was used as shown below:

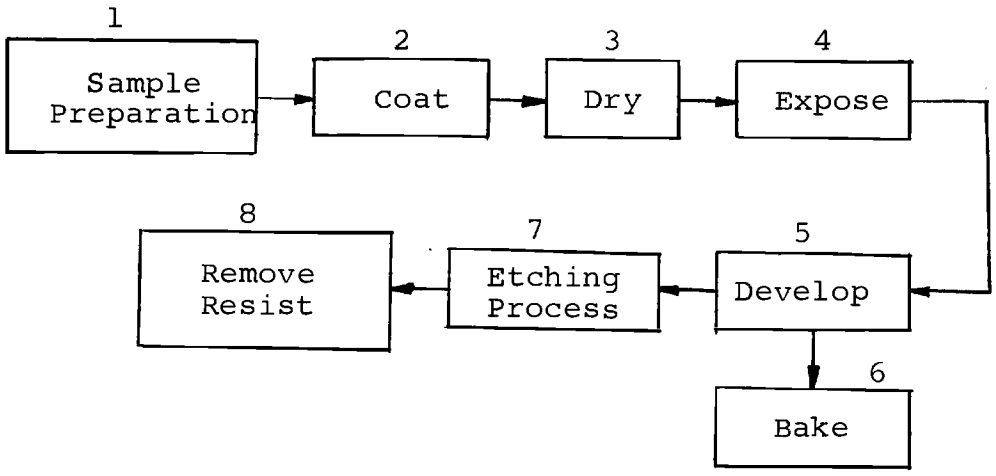

Figure 33. Flow diagram of the basic procedures of photolithographic techniques.

1. Sample Preparation. The initial preparation involves removing all foreign contaminants and traces of moisture from the Deltamax material as well as smoothing the surface, especially the edges and corners. Failure to do this can result in: (1) poor bonds between the KTFR and the Deltamax tape due to foreign particles and moisture from the surface of the sample; (2) irregular thickness of KTFR coating due to irregular surface, which results in irregular patterns during exposure; and (3) lifting of photoresist (KTFR) during etching process caused by penetration of etching acid solution at sharp edges and corners which failed to be coated properly.

The following procedures were followed in preparing the sample:

1. Make sure that the surfaces on both sides are smooth and all edges and corners are rounded.
2. Immerse the sample in boiling trichloroethylene (transistor grade) for approximately two minutes in order to remove all foreign contaminants from the sample.
3. Repeat step 2 in second bath of clean boiling trichloroethylene solution.
4. Dry under a 250 watt infrared lamp approximately 12 inches above the cleaned sample for 30 minutes in a dry atmosphere.

5. Cool in a desiccator before coating.

2. Coating KTFR. Basically two coating techniques are used: whirl coating and dip-coating. Spray coating may also be used to advantage on certain applications.

For best results the KTFR should be used as supplied (unthinned) and whirled just fast enough so the surface is uniform with no areas of excessive build up.

Apply the KTFR to the Deltamax tape as soon as possible after removal from the desiccator and turn on whirler at about 4000 RPM. Repeat a second time to assure complete and uniform coverage. Be sure to turn the sample around and repeat the same steps to the other side. Both sides must be coated.

3. Drying KTFR. Now that a uniform coating of KTFR has been applied, the coating must be dried (excess solvents removed). Failure to accomplish this may mean;

a. poor bonds to substrate
b. loss of acuity and resolution
c. loss of sensitivity
d. in extreme case the coating may stick to films and masks.

The coating can also be "overdried". This may result in;

a. loss of acuity and resolution
b. loss of sensitivity.

Fortunately there is a broad area between these extreme conditions where optimum results are obtained. The following technique was used: positioning a 250 watt infrared lamp approximately 12 inches above the part to be dried for approximately 20 minutes. Much of the drying took place in the whirler.

4. Exposure of KTFR. Select the slide with the desired pattern on it and place emulsion side down against the sample. Carefully align the pattern on the sample. Expose to ultraviolet light for approximately six to eight seconds. Optimum exposure time depends on many factors;

a. spectral output of light source
b. intensity of light
c. thickness of KTFR coating
d. absorption of light by system (glass, lens, film, etc.). In this case, it is the glass slide.

Note: To determine the optimum time for drying (step 3), exposure, and development (steps 4 and 5), a test should be made with a series of samples run at various times. The developed pieces showing the best acuity and resolution indicate the optimum time. The times mentioned in this paper do not necessarily represent the optimum timing.

5. Development of KTFR. Stoddard Solvent is used to develop KTFR. The development conditions and times, while not critical, should be controlled for optimum results. Optimum development time will vary to some extent on a number of factors, but will be determined chiefly by the thickness of the KTFR coating.

Using the spray gun containing Stoddard Solvent at a distance of approximately six inches, spray the sample until the desired pattern appears on the sample's surface. Rinse immediately after development. It will continue to develop until the developer is rinsed from the surface. Running deionized or tap water at 20°-25.5°C is best. The sample then should be dried.

6. Baking KTFR Coating. For resistance to strong chemical treatments such as HCl and HNO (nitric acid), baking is required. Baking is a time-temperature function: long times at moderate temperatures are equivalent to short times at high temperatures. Fifty minutes at 150°C (302°F) on a hot plate or under a sun lamp will enable KTFR images to resist the strong acid.

7. Etching Process. The etching solution for Deltamax (grain-oriented 50 percent nickel-iron alloy) is prepared by combining one part of HCl, one part of HNO_3 and three parts of H_2O. A ferric chloride solution can also be used.

Immerse the sample without agitation. It is probably best not to remove the sample frequently for inspection of progress. However, leaving it too long will eventually allow the etchant to crawl under the resist and cause poor definition of the pattern. A control sample is advised, which should be of the same material (Deltamax) and dimensions as the work piece, but without any photoresist coating on its surfaces. When the control sample is completely dissolved by the etching solution, the work piece should have its holes etched through, but due to small area of the holes it might take more time to etch through the Deltamax tape. Usually a minute or two after the control sample is completely dissolved, the work piece is removed for inspection.

8. Removal of KTFR from the Finished Sample. KTFR coating can be removed by boiling in trichloroethylene and scrubbing with a Q-tip.

A coating baked at high temperature for a long time, which is advisable (step 7), usually requires that the piece be heated to 60°C (140°F) in concentrated sulfuric acid H_2SO_4 for removal of the KTFR.

Conclusion

The procedures discussed in this Appendix were obtained partly from experimental results and partly

from the general instructions for using Kodak photoresist published by Eastman Kodak Company.

The results obtained were not entirely satisfactory. The working material was extracted from a Deltamax tape wound core; therefore the surface is not flat, it is curved. After it was flattened, the surfaces became inevitably irregular, so that during the coating operation the photoresist distributed unevenly on the sample's surfaces with areas of excessive build up and vice versa. This resulted in poor drying, exposure and development of the working sample.

A photomicrograph of a finished sample in Figure 3 shows that some holes are etched through, some partially etched, and some overetched, where the material around the hole is damaged. Note also that the shape of some of the holes is not perfectly round. These imperfections are caused by the nonuniform coating and distorted exposure produced by the irregular surfaces.

One of the main problems encountered in the etching process, and unfortunately unsolved, was the thickness reduction of the sample. A number of factors were responsible for this occurrence: (1) unclean sample surfaces, (2) improper drying time, development time, baking time and etching time. The author believes that factor number one is the main reason responsible for

poor bonding between the photoresist coating and sample surfaces, which caused the lifting of the coating and consequently caused the reduction of the sample thickness by acid during the etching process. The unclean surfaces come from the difficulty of removing completely the thick insulator emulsion with which the samples extracted from the tape-wound core were impregnated.

The problem which involves timing at different steps has already been discussed at each step. It was noted at step 4 that there is not a set or fixed optimum timing. The optimum timing should be determined by a series of tests. A complete run takes an average of three and one-half hours, which makes an accurate test a project in itself. The timing given at each step in this Appendix was the most accurate which could be determined from running a number of tests in the time available.

To improve the quality of the finished sample, the technique used at each step should be optimized by a series of tests, or the following alternative methods may be used: (1) Expose the KTFR coating on both sides of the Deltamax tape to the desired pattern and etch simultaneously both sides of the tape. To do this, a perfect alignment of patterns on both sides of the tape is necessary. (2) Double-coating technique (2, p. 19): KPR (Kodak Photo Resist) can be applied on KMER (Kodak

Metal-Etch Resist) coatings to produce thick photoresist images. It requires little exposure and less critical baking conditions than an equivalent thickness of KTFR.

Table II. Typical Characteristics for the Uncompensated, Apertured Deltamax Memory Cell.

I_R Ampere	uV_1 Millivolt	uV_Z Millivolt	$uV_Z@t_p$ Millivolt	t_s Microsecond	t_p Microsecond
0.1	4.0	4.0	4.0	2.40	0.20
0.2	7.0	4.0	4.0	2.20	0.20
0.3	11.0	8.0	7.0	2.00	0.20
0.4	16.0	12.0	9.0	1.85	0.18
0.5	20.0	14.0	12.0	1.65	0.15
0.6	25.0	17.0	14.0	1.50	0.15
0.7	30.0	21.0	19.0	1.35	0.15
0.8	35.0	25.0	22.0	1.30	0.15
0.9	43.0	27.0	24.0	1.20	0.10
1.0	50.0	30.0	27.0	1.20	0.10

Dimensions: Outer diameter = 0.052 inch Inner diameter = 0.008 inch
Thickness = 0.001 inch

Test Conditions: Ambient temp. = 25°C Write current = 800 ma
Write pulse width = 1 μsec Pulse rise time = 0.15 μsec
Pulse fall time = 0.10 μsec Frequency = 1 kilocycle

Variable Parameter: I_R = Read current

Measured Parameters: uV_1 = Uncompensated "undisturbed 1"
uV_Z = Uncompensated "undisturbed 0"
$uV_Z@t_p$ = "uncompensated "undisturbed 0" at t_p
t_p = Peaking time t_s = Switching time

Table III. Typical Characteristics for Compensated, Apertured Deltamax Memory Cell with a Read Current Pulse of One Ampere.

I_c Ampere	cV_1 Millivolt	cV_z Millivolt	$cV_z@t_p$ Millivolt	t_s Microsecond	t_p Microsecond
0.0	50.0	30.0	27.0	1.20	0.10
0.1	45.0	26.0	22.0	1.20	0.10
0.2	40.0	24.0	20.0	1.20	0.10
0.3	36.0	21.0	15.0	1.20	0.10
0.4	32.0	16.0	10.0	1.15	0.10
0.5	27.0	12.0	6.0	1.15	0.10
0.6	25.0	10.0	4.0	1.10	0.13
0.7	20.0	6.0	2.0	1.00	0.15
0.8	16.0	-6.0	-2.0	0.95	0.20
0.9	14.0	-9.0	-6.0	0.90	0.22
1.0	13.0	-13.0	-8.0	0.90	0.30

Dimensions: Outer diameter = 0.052 inch Inner diameter = 0.008 inch
Thickness = 0.001 inch

Test Conditions: Ambient temp. = 25°C Write current = 1 ampere
Write pulse width = 1 μsec
Read current = 800 ma Read pulse width = 2 μsec
Pulse rise time = 0.15 μsec
Pulse fall time = 0.10 μsec Frequency = 1 kilocycle

Variable Parameter: I_c = Compensation current

Measured Parameters: cV_1 = Compensated "undisturbed 1"
cV_z = Compensated "undisturbed 0"
$cV_z@t_p$ = Compensated "undisturbed 0" at t_p

t_p = Peaking time t_s = Switching time

Table IV. Typical Characteristics for the Compensated, Apertured Deltamax Memory Cell with a Read Current Pulse of 800 Milliamperes.

I_c Ampere	cV_1 Millivolt	cV_z Millivolt	$cV_z@t_p$ Millivolt	t_s Microsecond	t_p Microsecond
0.0	35.0	25.0	22.0	1.30	0.15
0.1	31.0	21.0	15.0	1.30	0.15
0.2	28.0	18.0	10.0	1.30	0.15
0.3	24.0	12.0	6.0	1.30	0.15
0.4	22.0	9.0	4.0	1.30	0.18
0.5	18.0	6.0	3.0	1.25	0.20
0.6	17.0	5.0	0.0	1.20	0.25
0.7	13.0	4.0	-2.0	1.10	0.28
0.8	12.0	-5.0	-4.0	1.05	0.30
0.9	10.0	-10.0	-6.0	1.00	0.32
1.0	10.0	-13.0	-8.0	1.00	0.40

Dimensions: Outer diameter = 0.052 inch; Write pulse width = 1 μsec; Read pulse width = 2 μsec; Pulse fall time = 0.10 μsec; Write current = 800 ma; Read current = 800 ma; Pulse rise time = 0.15 μsec; Frequency = 1 kilocycle

Variable Parameter: I_c = Compensation current

Measured Parameters: cV_1 = Compensated "undisturbed 1"
cV_z = Compensated "undisturbed 0"
$cV_z@t_p$ = Compensated "undisturbed 0" at t_p
t_p = Peaking time t_s = Switching time

Table V. Typical Characteristics for Compensated, Apertured Deltamax Memory Cell with a Read Current Pulse of 500 Milliamperes.

I_c Ampere	cV_1 Millivolt	cV_z Millivolt	$cV_z@t_p$ Millivolt	t_s Microsecond	t_p Microsecond
0.0	20.0	14.0	12.0	1.65	0.15
0.1	13.0	9.0	7.0	1.65	0.15
0.2	11.0	7.0	4.0	1.65	0.18
0.3	9.0	4.0	3.0	1.60	0.22
0.4	7.0	-	0.0	1.55	0.27
0.5	6.0	-5.0	-1.0	1.52	0.35
0.6	5.0	-7.0	-2.0	1.50	0.40
0.7	5.0	-10.0	-2.0	1.50	0.45
0.8	4.0	-13.0	-4.0	1.45	0.50
0.9	3.0	-14.0	-5.0	1.42	0.58
1.0	3.0	-15.0	-6.0	1.40	0.60

Dimensions: Outer diameter = 0.052 inch Inner diameter = 0.008 inch
Thickness = 0.001 inch

Test Conditions: Ambient temp. = 25°C Write current = 800 ma
Write pulse width = 1 μsec
Read current = 500 ma Read pulse width = 2 μsec
Pulse rise time = 0.15 μsec Pulse fall time = 0.10 μsec
Frequency = 1 kilocycle

Variable Parameter: I_c = Compensation current

Measured Parameters: cV_1 = Compensated "undisturbed 1"
cV_z = Compensated "undisturbed 0"
$cV_z@t_p$ = Compensated "undisturbed 0" at t_p
t_p = Peaking time t_s = Switching time

Table VI. Variation of Typical Characteristics for the Compensated, Apertured Deltamax Memory Cell with Write Current (I_w).

I_w Ampere	cV_1 Millivolt	cV_z Millivolt	$cV_z@t_p$ Millivolt	t_s Microsecond	t_p Microsecond
0.0	7.0	6.0	5.0	0.35	0.15
0.1	7.0	6.0	5.0	0.35	0.15
0.2	7.5	6.0	5.0	0.45	0.15
0.3	10.0	6.0	5.0	0.55	0.15
0.4	12.0	6.0	5.0	0.68	0.15
0.5	14.5	6.0	5.0	0.80	0.15
0.6	15.5	6.0	5.0	0.90	0.15
0.7	17.0	6.0	5.0	1.05	0.15
0.8	18.0	6.0	3.0	1.25	0.20
0.9	18.0	6.0	3.0	1.25	0.20
1.0	18.0	6.0	3.0	1.25	0.20

Dimensions: Outer diameter = 0.052 inch Inner diameter = 0.008 inch
Thickness = 0.001 inch

Test Conditions: Ambient temp. = 25°C Read current = 800 ma
Read pulse width = 2 μsec Compensation current = 500 ma
Pulse rise time = 0.15 μsec Pulse fall time = 0.10 μsec
Frequency = 1 kilocycle

Variable Parameter: I_w = Write current

Measured Parameters: cV_1 = Compensated "undisturbed 1"
cV_z = Compensated "undisturbed 0"
$cV_z@t_p$ = Compensated "undisturbed 0" at t
t_p = Peaking time t_s = Switching time

Table VII. Variation of the Typical Characteristics for the Compensated, Apertured Deltamax Memory Cell with Write Pulse Width (t_d).

t_d Microsecond	cV_1 Millisecond	cV_z Millivolt	$cV_z@t_p$ Millivolt	t_s Microsecond	t_p Microsecond
0.1	7.0	6.0	5.0	0.40	0.10
0.2	8.5	6.0	5.0	0.50	0.10
0.3	11.5	6.0	5.0	0.65	0.10
0.4	14.0	6.0	5.0	0.80	0.10
0.5	16.0	6.0	4.0	0.90	0.14
0.6	17.0	6.0	3.0	1.00	0.20
0.7	17.0	6.0	3.0	1.10	0.20
0.8	18.0	6.0	3.0	1.20	0.20
0.9	18.0	6.0	3.0	1.25	0.20
1.0	18.0	6.0	3.0	1.25	0.20

Dimensions: Outer diameter = 0.052 inch Inner diameter = 0.008 inch
Thickness = 0.001 inch

Test Conditions: Ambient temp. = 25°C Write current = 800 ma
Read current = 800 ma Compensation current = 500 ma
Read pulse width = 2 μsec Pulse rise time = 0.15 μsec
Pulse fall time = 0.10 μsec Frequency = 1 kilocycle

Variable Parameter: t_d = Write pulse width

Measured Parameters: cV_1 = Compensated "undisturbed 1"
cV_z = Compensated "undisturbed 0"
$cV_z@t_p$ = Compensated "undisturbed 0" at t_p
t_p = Peaking time t_s = Switching time

Table VIII. Temperature Effect on the Response of the Compensated, Apertured Deltamax Memory Cell.

T Degrees Fahrenheit	cV_1 Millivolt	cV_Z Millivolt	$cV_Z@t_p$ Millivolt	t_s Microsecond	t_p Microsecond
-75°	13.0	3.0	0.0	1.20	0.32
-50°	13.0	3.5	0.0	1.20	0.3
-25°	14.0	4.0	0.0	1.15	0.28
0°	15.0	4.0	0.0	1.15	0.25
75°	17.0	5.0	0.0	1.10	0.25
100°	17.0	5.0	0.0	1.10	0.22
150°	18.0	5.0	0.0	1.10	0.20
200°	19.0	5.0	1.0	1.10	0.20
250°	20.0	5.5	1.0	1.08	0.18
300°	21.5	6.0	1.5	1.08	0.18
350°	24.0	7.0	2.0	1.05	0.15
400°	24.5	8.0	3.0	1.05	0.18
425°	25	8.5	3.0	1.05	0.15

Dimensions: Outer diameter = 0.052 inch Inner diameter = 0.008 inch
Thickness = 0.001 inch

Test Conditions: Ambient temp. = 25°C Write current = 800 ma
Write pulse width = 1 μsec
Read current = 800 ma Compensation drive = 600 ma
Read pulse width = 2 μsec
Pulse rise time = 0.15 μsec Pulse fall time = 0.10 μsec

Variable Parameter: T = Tested temperature

Measured Parameters: cV_1 = Compensated "undisturbed 1" t_p = Peaking time
cV_Z = Compensated "undisturbed 0" t_s = Switching time
$cV_Z@t_p$ = Compensated "undisturbed 0" at t_p

Table IX. Temperature Effect on the RCA Type 226M1 Ferrite Core.

T Degrees Fahrenheit	uV_1 Millivolt	uV_Z Millivolt	$uV_Z@t_p$ Millivolt	t_s Microsecond	t_p Microsecond
-75°	140.0	20.0	0.0	0.55	0.35
-50°	180.0	20.0	0.0	0.52	0.33
-25°	220.0	20.0	0.0	0.50	0.30
0°	240.0	20.0	0.0	0.46	0.28
75°	290.0	20.0	5.0	0.37	0.23
100°	310.0	20.0	7.0	0.35	0.22
150°	330.0	25.0	8.0	0.30	0.18
200°	350.0	28.0	10.0	0.25	0.15
250°	370.0	35.0	12.0	0.22	0.12
300°	350.0	40.0	15.0	0.20	0.10
350°	320.0	50.0	20.0	0.18	0.08
400°	150.0	35.0	25.0	0.13	0.06
425°	0.0	0.0	0.0	0.08	0.05

Dimensions: Outer diameter = 0.050 inch Inner diameter = 0.030 inch
Thickness = 0.015 inch

Test Conditions: Ambient temp. = 25°C Read current = 800 ma
Read pulse width = 1 μsec
Write current = 800 ma Write pulse width = 1 μsec
Pulse rise time = 0.15 μsec Pulse fall time = 0.10 μsec

Variable Parameter: T = Tested temperature

Measured Parameters: uV_1 = "Undisturbed 1"
uV_Z = "Undisturbed 0"
$uV_Z@t_p$ = "Undisturbed 0" at t_p

t_p = Peaking time t_s = Switching time